

Fl
12

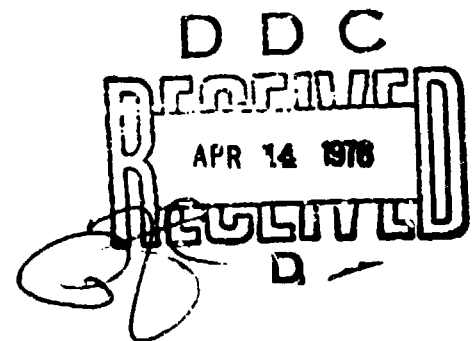
PAPER P-1137

**ANALYSIS OF BOUNDARY LAYER TRANSITION EFFECTS
ON BALLISTIC REENTRY VEHICLE IMPACT DISPERSION
AND COMPARISON WITH OTHER DISPERSION FACTORS**

H. P. Liepman

December 1975

AD A 022949



INSTITUTE FOR DEFENSE ANALYSES
SCIENCE AND TECHNOLOGY DIVISION

DISTRIBUTION STATEMENT A
Approved for public release;
Distribution Unlimited

IDA Log No. HQ 75-17634
Copy 55 of 75 copies

Reference of
for letter
R# 4-13-76

The work reported in this document was conducted under Contract DAHC15 73 C 0200 for the Department of Defense. The publication of this IDA Paper does not indicate endorsement by the Department of Defense, nor should the contents be construed as reflecting the official position of that agency.

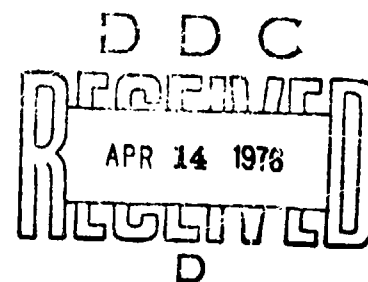
Approved for public release; distribution unlimited.

PAPER P-1137

ANALYSIS OF BOUNDARY LAYER TRANSITION EFFECTS ON BALLISTIC REENTRY VEHICLE IMPACT DISPERSION AND COMPARISON WITH OTHER DISPERSION FACTORS

H. P. Liepman

December 1975



INSTITUTE FOR DEFENSE ANALYSES
SCIENCE AND TECHNOLOGY DIVISION
400 Army-Navy Drive, Arlington, Virginia 22202

Contract DAHC15 73 C 0200
Task T-108

ACCESSION for	
NTIS	White Section <input checked="" type="checkbox"/>
DDC	Buff Section <input type="checkbox"/>
UNCLASSIFIED	<input type="checkbox"/>
JUSTIFICATION	
BY	
DISTRIBUTION/AVAILABILITY CODES	
Dist.	AVAIL. and/or SPECIAL
A	

DISTRIBUTION STATEMENT A
Approved for public release;
Distribution Unlimited

UNCLASSIFIED

SECURITY CLASSIFICATION OF THIS PAGE (When Data Entered)

REPORT DOCUMENTATION PAGE		READ INSTRUCTIONS BEFORE COMPLETING FORM
1. REPORT NUMBER Paper P-1137	2. GOVT ACCESSION NO.	3. RECIPIENT'S CATALOG NUMBER
4. TITLE (and Subtitle) Analysis of Boundary Layer Transition Effects on Ballistic Reentry Vehicle Dispersion and Comparison with Other Dispersion Factors.	5. AUTHOR H. P. Liepman	6. TYPE OF REPORT & PERIOD COVERED Final report May - Dec 1975
7. PERFORMING ORGANIZATION NAME AND ADDRESS Institute for Defense Analyses 400 Army-Navy Drive Arlington, Virginia 22202	8. CONTRACT OR GRANT NUMBER(s) DAHC-15-73-C-0200	9. PERFORMING ORG. REPORT NUMBER P-1137
10. CONTROLLING OFFICE NAME AND ADDRESS Defense Advanced Research Projects Agency 1400 Wilson Boulevard Arlington, Virginia 22209	11. PROGRAM ELEMENT PROJECT TASK AREA & WORK UNIT NUMBERS Task T-103	12. REPORT DATE December 1975
13. MONITORING AGENCY NAME & ADDRESS (if different from Controlling Office) AD (Engineering Technology), R&AT, ODDR&E	14. NUMBER OF PAGES 47	15. SECURITY CLASS (of this report) UNCLASSIFIED
16. DISTRIBUTION STATEMENT (of this Report) Approved for public release; distribution unlimited.		17. SECURITY CLASS (of this report) UNCLASSIFIED
18. DISTRIBUTION STATEMENT (of the abstract entered in Block 20, if different from Report) None		19. DECLASSIFICATION DOWNGRADING SCHEDULE
20. SUPPLEMENTARY NOTES None		
21. KEY WORDS (Continue on reverse side if necessary and identify by block number) boundary layer transition, impact dispersions, ballistic reentry vehicles, ballistic		
22. ABSTRACT (Continue on reverse side if necessary and identify by block number) This paper analyzes the impact dispersion of a ballistic reentry vehicle caused by the transitory lift and drag components encountered during the brief altitude regime where the vehicle's boundary layer is changing from laminar to turbulent behavior. A simple physical model of the phenomenon is developed using adjustable parameters since the basic aerothermal materials physics is poorly understood. The adjustable parameters are identifiable with physical assumptions and one result is		

DD FORM 1 JAN 73 1473 EDITION OF 1 NOV 68 IS OBSOLETE

UNCLASSIFIED
SECURITY CLASSIFICATION OF THIS PAGE (When Data Entered)

403 108

UNCLASSIFIED


SECURITY CLASSIFICATION OF THIS PAGE (When Data Entered)

Item 20 (Continued)

to focus attention on the nature of these assumptions in order to guide further theoretical and experimental work which can develop a better understanding of the phenomenon, particularly its impact on materials and structures technology.

Under the assumptions made, numerical estimates are made of the boundary layer transition dispersion for a practical range of vehicle and trajectory parameters, and then compared with contributions from density, wind velocity, and drag variations and from the roll-through-zero effect. The boundary layer effects are found to be too large to be ignored and further studies are needed to bound the behavior.

Additional studies of the Materials and Structures Technology Base Programs related to reentry vehicle mission requirements will be made in a subsequent paper.



UNCLASSIFIED

SECURITY CLASSIFICATION OF THIS PAGE (When Data Entered)

ACKNOWLEDGMENTS

The author gratefully acknowledges the contributions made by L. S. Glover of the Applied Physics Laboratory, Johns Hopkins University, and by V. J. Berinati, E. L. Foster, J. E. Hove, and W. J. Schultis of the IDA staff through their many constructive discussions and comments as reviewers.

ABSTRACT

This paper analyzes the impact dispersion of a ballistic reentry vehicle caused by the transitory lift and drag components encountered during the brief altitude regime where the vehicle's boundary layer is changing from laminar to turbulent behavior. A simple physical model of the phenomenon is developed using adjustable parameters since the basic aerothermal materials physics is poorly understood. The adjustable parameters are identifiable with physical assumptions and one result is to focus attention on the nature of these assumptions in order to guide further theoretical and experimental work which can develop a better understanding of the phenomenon, particularly its impact on materials and structures technology.

Under the assumptions made, numerical estimates are made of the boundary layer transition dispersion for a practical range of vehicle and trajectory parameters, and then compared with contributions from density, wind velocity, and drag variations and from the roll-through-zero effect. The boundary layer effects are found to be too large to be ignored and further studies are needed to bound the behavior.

Additional studies of the Materials and Structures Technology Base Programs related to reentry vehicle mission requirements will be made in a subsequent paper.

SUMMARY

A. PURPOSE AND SCOPE

The Office of the Deputy Director (Research and Advanced Technology), ODDR&E, has, under DARPA Task Order T-106, requested the Institute for Defense Analyses to carry out a study of the Materials and Structures Technology Base Programs.

The present paper is a partial input to that portion of this study pertaining to the overall ballistic missile reentry vehicle (RV) mission requirements. A more complete study of the tradeoffs between stated RV mission requirements and materials/structures capabilities and properties, together with an assessment of the scopes and efforts of the present Technology Base Programs, will be presented in a subsequent report. Before such a study can become meaningful, however, the various effects that can contribute to the diminished success of an RV mission should be known in as quantitative a manner as possible. One effect, which could make a significant contribution to the RV impact dispersion from the target, involves the forces (particularly the asymmetric forces) induced on the RV by the boundary layer transition (BLT) dynamics during the altitude interval where laminar flow becomes turbulent over the RV surface.

The purpose of the present paper is to analyze the potential contribution of the BLT effects to the inaccuracy of the RV ballistic trajectory, and to make quantitative comparisons with other effects, in clear air and in the absence of hostile defensive action. Although the results necessarily contain uncertainties due to the lack of a thorough basic understanding of the phenomenon itself, or (more precisely) its dynamic

behavior as affected by the RV materials and flight parameters, this analysis is a first attempt to put the BLT effects on vehicle performance into a simplified mathematical framework that can highlight the importance of the various parameters and thus guide future R&D on materials and structures for RVs.

B. METHOD OF ANALYSIS

Because the various BLT phenomena are complex and poorly understood, certain assumptions must be made. One is the width of the altitude layer in which occur the transition and the associated transitory increments of drag and lift. The layer width can be deduced, within reasonable bounds, by flight and ground-facility tests. The induced aerodynamic effects, particularly the incremental lift, are more difficult to estimate. In the analysis, the lift increment is replaced (together with known aerodynamic and geometric characteristics) by the BLT moment coefficient increment, whose range of values has been given in the literature. This range is large in both flight-derived and wind tunnel data (a factor of 10 variation is common). The value used in this analysis is the low end of the wind tunnel data, which corresponds to the average value for the flight-test estimates.

Another, somewhat simplistic, assumption relates to the length of time the induced asymmetric lift vector remains in the plane of the trajectory. Clearly, if this vector rotated circumferentially at a greatly different rate than the roll rate of the vehicle, the effects would be greatly diminished and could become insignificant. Conversely, if it remained fixed in the trajectory plane during the entire transition region, the adverse effects would be very great. Since it is believed from flight-test analyses that an appreciable effect does indeed exist, an educated estimate was made for this factor. If later evidence should indicate a change in the numerical estimate, a simple means is presented to scale the results

appropriately. In any case, the need is obvious for further study to better understand the dynamic interplay between material roughening and shape change, the vehicle aerothermal and aerodynamic factors, and the transition edge motion on the vehicle surface.

It should be pointed out that the above assumption, that the BLT-induced lift vector stays for an appreciable time in the trajectory plane, implies a worst-case analysis since all the dispersion will be up- or down-range. In general, this lift plane will lie between the down- and cross-range directions and its contribution to CEP will be less than the worst case. The method for handling this more general behavior is shown, but the calculations are only made for the worst case.

The method of analysis uses an adaptation of the equations of Glover and Hagan (Ref. 6) with which they analyzed the roll-through-zero (RTZ) dispersions. The final BLT equation is put in a form where the altitude of transition is one of the independent variables, along with the ballistic coefficient and the angle of reentry. The velocity of reentry, incidentally, drops out of the equation.

The numerical BLT asymmetric dispersion effects (in the worst-case mode) are first calculated (in Section II) for several ballistic coefficients and reentry angles as a function of the transition altitude. The values for two altitudes (45 and 100 kft) are then replotted (in Section III) against reentry angles for three ballistic coefficients (1000, 2000, and 3000 psf) and graphically compared with the conventional and roll-through-zero components of dispersion. The latter two are dependent on the reentry velocity (which BLT effects are not), and a velocity of 20,000 fps is used with a variation spread shown for 16,000 and 24,000 fps (which shows only a small deviation). Finally, for the sake of completeness and clarity, the roll-through-zero and the boundary layer transition maximum

dispersions are plotted in various ways as a fraction of the conventional dispersion component (i.e., root-mean-square values of the effects of density, wind, and drag variations).

C. RESULTS

1 General Results

a. For practical altitudes of interest (30 to 100 kft), a transition altitude of about 45 kft gives the maximum BLT dispersion effect, regardless of other influences. From this standpoint, it is advantageous to induce transition at altitudes either considerably above or below 45,000 ft and, in fact, the preponderance of present transition altitudes occurs above this value. However, a penalty is paid for higher transition altitudes in that they lead to longer periods of turbulent heat transfer. This has two undersirable effects: first, and more important, it causes greater ablation rates and shear stresses for longer times and thus increases the recession and shape change of the tip and heat shield (also note that surface roughening tends to greatly enhance the already high turbulent heating and amplifies the adverse material effects); second, a turbulent wake yields a higher radar signature which makes the vehicle easier to see at higher altitudes. Therefore, there is a distinct advantage to maintaining laminar flow well below 45,000 ft for more reasons than the BLT effect only. Such low transition altitudes have been achieved repeatedly using advanced materials and different tip designs (see Ref. 7).

b. The BLT maximum dispersion is a strong function of the reentry angle, varying inversely as the third power of its sine regardless of the altitude of transition. In a qualitative way, conventional and roll-dynamic dispersion behave similarly with reentry angle, although not as strongly. Thus, from the viewpoint of impact dispersion, it is desirable to loft the vehicle

and come in at as steep a reentry path as the boost energy will allow. However, this will result in increased heating rates, stagnation pressures, shear stresses, and other environmental factors which may exceed the material limits.

c. The BLT dispersion varies inversely as the ballistic coefficient and static margin. As in the reentry angle case, all the dispersion contributions considered here quantitatively behave similarly. The same argument follows: from an impact dispersion standpoint, the higher ballistic coefficients are more desirable, but the materials/structures problems (of simply reaching the ground) become more severe. And increasing the static stability margin imposes severe weight penalties on the RV. Thus, tradeoff studies are necessary, including the effects of particle erosion which are ignored herein and will be discussed in a follow-on report.

2. Specific Numerical Results

Calculations were made for a slender sphere-cone vehicle with a 7 percent static margin and a transition-induced asymmetrical moment coefficient of 0.001 (see Section B of this Summary). This moment coefficient is equivalent to a 0.15-deg trim angle of attack. The induced moment (or lift vector) is assumed to act in the plane of the trajectory for half the period of the boundary layer transition time. The altitude delta for transition to occur is taken as 10 percent of the transition altitude. With these assumptions, the following results are obtained (summarized from the various curves presented in the report).

a. Maximum BLT impact dispersions are shown of the order of 25-1000 ft for ballistic coefficients from 3000-1000 psf and reentry angles from 50 to 20 deg, respectively, for the asymmetric modes. The effects of the symmetric modes are small by comparison, and can be ignored. This is to be compared with a maximum roll-through-zero impact dispersion of 150-2000 ft for the same range of ballistic coefficients and reentry angles.

The final comparison is with the conventional dispersion components, which range from 35-3500 ft for these extrema of parameters. To give an illustrative specific example, let us use a ballistic coefficient of 2000, reentry angle of 30 deg, and a reentry velocity of 20,000 fps. The rangewise dispersion is about 180 ft for the conventional component, 150 ft for maximum BLT, and 550 ft for maximum roll-through-zero. If these are simply added, the maximum dispersion would be about 880 ft. Using the assumption that these components can be root-sum-squared, the maximum dispersion would be about 600 ft. If there is no RTZ, this figure becomes 240 ft. Since a root-sum-square treatment may be too simplified, all that can be said is that the maximum BLT effects (by themselves) can increase the normal dispersion component by approximately 30-80 percent for this specific case.

These results indicate that the maximum asymmetric BLT dispersion effects appear to be somewhat smaller than, but of the same order as, the conventional dispersion effects. Thus, the boundary layer transition dispersion cannot be ignored at this stage of our knowledge. Clearly, an improved theoretical and experimental data base is needed to bound the phenomenon, particularly as it is affected by the contributions of RV surface roughening, ablative blowing, shape changes, nose-tip design, and trajectory parameters.

CONTENTS

Acknowledgments	11
Abstract	111
Summary	iv
I. INTRODUCTION	1
II. BOUNDARY LAYER TRANSITION DISPERSION EFFECTS	3
A. Background	3
B. Boundary Layer Transition	4
C. Impact Dispersions Due to Boundary Layer Transition	9
D. Discussion	23
III. IMPACT DISPERSION ESTIMATES	29
A. Background	29
B. Conventional Dispersion Components	30
C. Roll-Dynamics Dispersion Components	32
D. Boundary Layer Transition Dispersion Components	36
E. Combined Dispersions	38
F. Dispersion Ratios Relative to the Conventional Dispersion	40
References	46

I. INTRODUCTION

Aside from problems related to guidance and the release mechanism of the delivery system, the accuracy and reliability of a ballistic reentry vehicle (RV) is a complex and interactive function of its aerodynamic and thermal environment and its overall materials, structural, and design properties. To this must be added manufacturing and assembly reliability as it affects the offset of the center of gravity or center of pressure, lack of uniformity in material properties, and a number of other factors. Even ignoring hostile defensive actions (which will be done throughout this paper), the difficulties in achieving an acceptably small circular error probability (CEP) of impacting a target are not well understood in a quantitative manner.

The ultimate factor limiting the options open to the RV designer is the availability of materials for the nose tip, the heat shield, and the substructure. These limitations thus dictate the military operational capabilities regarding the ballistic coefficient, the reentry-velocity-angle map, etc., both from the standpoint of whether the RV will actually reach impact and of its accuracy. The various tradeoffs between mission requirements and the materials/structures (M/S) technologies available or under study, as well as an assessment of the scopes and efforts of the M/S Technology Base Programs in support of reentry vehicles, will be the subject of another report.

Before a meaningful study can be made of the present and contemplated M/S programs, it becomes essential to first analyze

the various factors affecting RV impact dispersion, even if the basic phenomena are not well understood. This points out the areas where future R&D are most required on the basis of the assumptions made. It will also focus attention on the critical assumptions themselves, which require better resolution.

It is important to specifically list the areas that are not included in this report. These are:

- Burnthrough, tumbling, and other factors that could lead to premature structural breakup, premature fuzing, or other major events that completely abort the mission
- Hostile defensive action
- RV maneuverability, although the analysis of methodology could contribute, and
- Erosion due to rain, snow, ice, or dust particles.

Three dispersion effects are considered:

- Uncertainties in wind, density, and symmetric drag, all of which are root-mean-squared to arrive at their CEP contribution
- Roll-trim dynamics, including roll-through-zero, and
- Boundary layer transition effects.

The major contribution of this paper is to develop a simple physical model of the boundary layer transition effects on the trajectory and calculate quantitative impact dispersion contributions for various ballistic coefficients and reentry parameters of practical interest. These contributions are then compared with those of the other two dispersion effects and presented both in an absolute sense and a relative sense. The significance of these findings for R&D on materials and structures will be considered in another paper.

II. BOUNDARY LAYER TRANSITION DISPERSION EFFECTS

A. BACKGROUND

Recent analyses of flight data (Ref. 1) have indicated that the boundary layer transition gives asymmetric aerodynamic perturbations with a strong impact on the flight dynamics of reentry vehicles. These new data come on top of our slowly developing understanding of interactions between severe nose-shape changes and the development and progression of the transition phenomenon on the tip itself. In addition, the development of advanced tip and frustum heat protection materials recognizes a strong interplay between initiation of transition by the ablative (blowing, charring, melting, etc.) and local roughness characteristics of the material. A desirable material, then, should allow the following behaviors: the onset of transition should be delayed as long as possible, the transition process should remain repeatable and produce stable nose shapes, and the roughness of the ablating material should be minimal to keep local heating augmentation small.

The effects of boundary layer transition on the accuracy of the ballistic trajectory are of interest here. A simple physical picture of the transition process is combined with reasonable approximations of the trajectory to bound the target dispersion due to transition at various altitudes.

Section II.B develops the simple physical model of transition used subsequently. The approximate equations for impact dispersions are developed in Section II.C in two parts. One deals with the symmetric aspects of transition, which are evidenced by an effective drag increment over a finite interval

above and below the nominal altitude of transition. The other part is due to the aerodynamic asymmetry of transition remaining in the trajectory plane for a small but finite portion of the transition period. This latter part of impact dispersions due to transition-induced asymmetries is analogous to the roll-through-zero phenomenon of aerodynamic and mass asymmetries together with the coupling of angular rates. The implications of the results on reentry vehicle design and trajectory shaping are discussed in Section II.D.

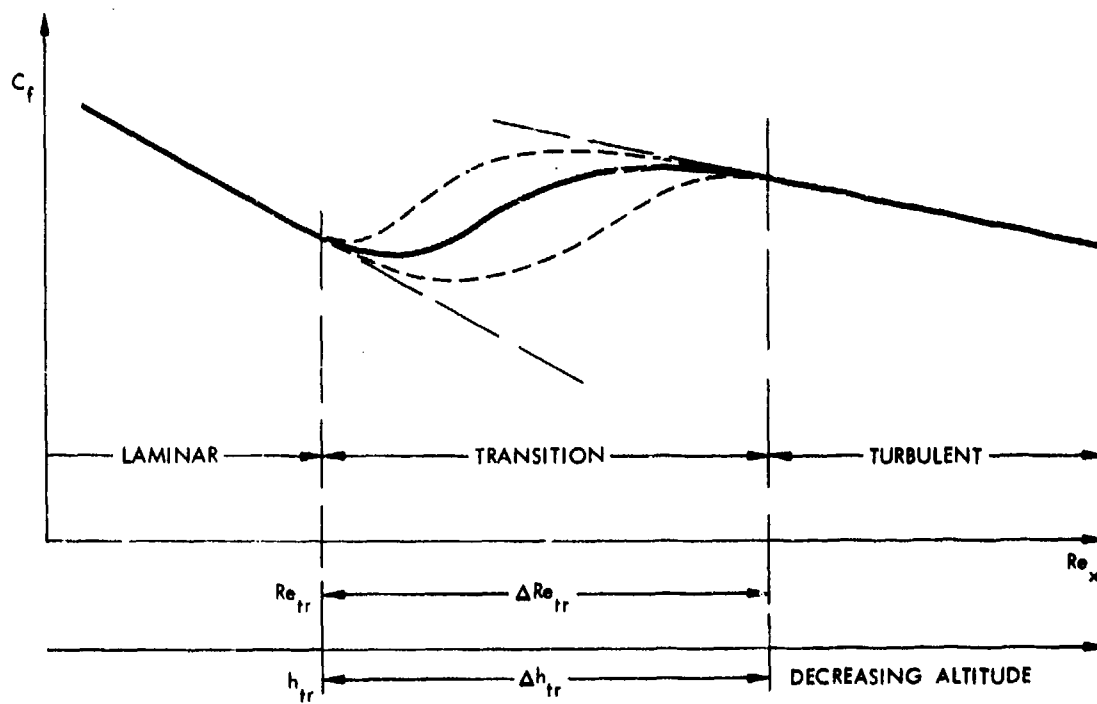
B. BOUNDARY LAYER TRANSITION

Boundary layer transition (BLT), especially on hypersonic ablating reentry vehicles (RVs), has been a persistent, practical and theoretical puzzler (for instance, Ref. 2). The occurrence is an obvious and well-known fact. However, the complex interactions of all the participating and interacting contributors still limit our understanding and predictability of BLT on RVs to the art of empirical correlation instead of advancing to a physically consistent model with broad experimental validations.

Relating BLT to impact dispersions requires first a description of the physical characteristics we ascribe to the transition process. Only an elementary description of transition is given here to set the stage for the analyses to follow and to introduce transition-related parameters.

As the RV descends through the atmosphere some altitude h_{tr} is reached at which the character of the viscous flow in the boundary layer around the body begins to deviate from its laminar character. Transition to a fully turbulent boundary layer takes place over a finite altitude interval, Δh_{tr} . The transition altitude h_{tr} , thus defined, corresponds to a Reynolds number based on a body length ($Re_x = \rho Vx/\mu$) exceeding a critical value Re_{tr} . The transition interval Δh_{tr} corresponds to an increment ΔRe_{tr} defined such that fully turbulent flow is achieved at

$Re_{tr} + \Delta Re_{tr}$. Figure 1 shows a sketch of the frictional drag coefficient versus Reynolds number. The dashed lines indicate representative envelopes of possible transition curves. Transition may depart slowly or rapidly from its laminar state and may approach the fully turbulent state rapidly or slowly in a random, unpredictable manner. The onset, h_{tr} , and completion, $(h_{tr} + \Delta h_{tr})$, of transition are equally subject to uncertainties. This will be taken into account later in this section.



12-8-75-4

FIGURE 1. Boundary Layer Transition Terminology

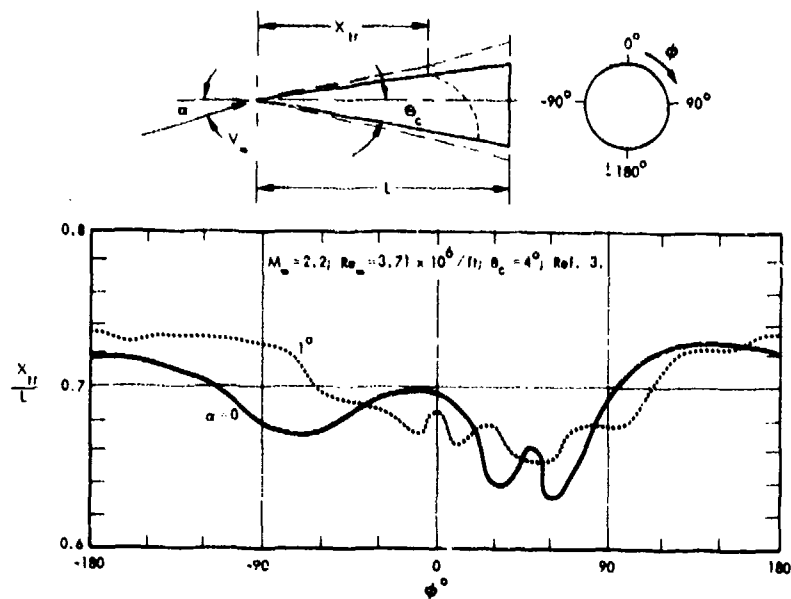
Once the transition has begun (usually at the base of the RV), the forward edge of transition, the transition front, will move in a highly unpredictable manner. The front can move fore and aft (a local relaminarization) or it can move around the body and these movements can be at various rates including, for instance, a very rapid flashing forward all the way to the nose region or around the body in a spiral mode. The location and

motion of the transition front appear to be affected by many interrelated parameters, of which the most prominent ones are (at least according to our current naive understanding of the phenomenon): angle of attack (large and small; even less than one degree has been seen to be effective in transition-front movement); nose radius bluntness ratio through its entropy gradient interaction with the boundary layer (entropy swallowing location); initial and ablating surface roughness distributions; ablative blowing, cross-hatching, and shape changes; pressure gradients; temperature ratios; and others.

The circumferential distribution of the transition front has received the least attention as to its characteristics, its forcing parameters, and its potential angular rate, but it has the greatest impact on dispersion, as will be seen later. Figure 2 shows typical static circumferential variations of transition fronts at various angles of attack on wind tunnel models of 4-deg and 8-deg half-angle cones with sharp noses (Refs. 3 and 4). Note that even at $\alpha = 0$ (Fig. 2a) there are transition tongues at $\phi = 30$ and 60 deg that might rotate around the body in response to a nonuniform pressure distribution.

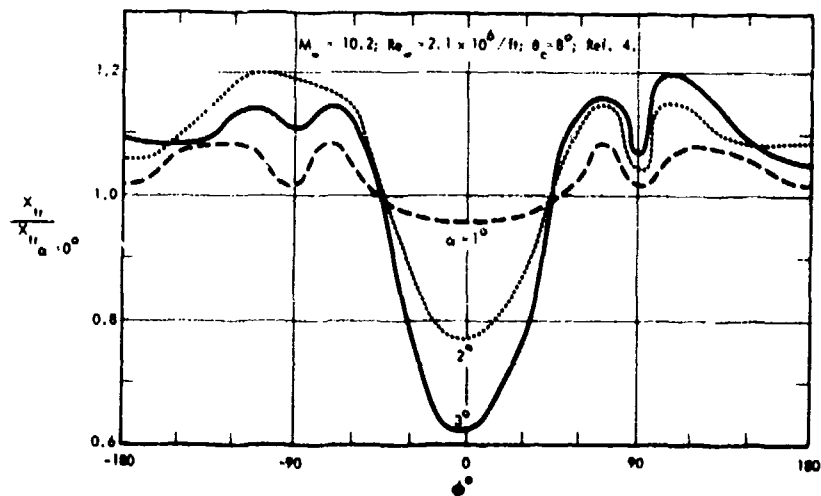
One other characteristic of the transition process should be kept in mind, namely its fundamentally random character. Significant temporal and spatial variations about the mean location of the transition front (or any other transition-related parameter) are to be expected and no single "design" value can be used to describe the transition effects. Furthermore, the statistical characterization of transition under hypersonic flow conditions is not at all clear in view of the many interacting parameters that can attenuate or amplify the perturbations leading to transition.

In this discussion, the onset of transition has been associated with a transition altitude h_{tr} . Other definitions of this transition altitude are equally valid, such as when turbulent flow is reached or at some intermediate situation. This



12-6-75-1

(a)



12-6-75-2

(b)

FIGURE 2. Typical Circumferential Location of Transition for Two Sharp Cones in Wind Tunnels

is not terribly important as long as it is recognized that, whatever the defining convention for h_{tr} is, it represents only a mean value h_{tr} , and that the transition phenomenon could occur anywhere within a statistically meaningful altitude interval, say $h_{tr} \pm \Delta h_{tr}$.

During boundary layer transition, the reentry body experiences major changes in aerodynamic forces and moments and a significant increase in convective heat transfer. The skin friction component of total drag increases as the boundary layer changes from laminar to turbulent. Concurrently, the slope of the edge of the boundary layer increases, thus increasing the effective slope of the body (displacement-thickness concept) and the inviscid flow acts on this effective body flare by producing a local pressure increment. It is most unlikely that this pressure increment is completely symmetric; hence, aerodynamic asymmetry, a lift and moment increment, and an associated trim angle of attack will result. The increasing convective heat transfer increases ablation and blowing, which in turn amplify the strength of the effective flare introduced by the region of boundary layer transition. The heat-transfer-induced amplifications of aerodynamic forces and moments during BLT are thus a strong function of the ablation rate of the heat shield material and the degree of severity of the reentry environment defined by the reentry velocity and reentry angle.

The effects of this complex and poorly understood boundary layer transition process or dispersion will be treated in two parts. One, a symmetric component, takes all BLT effects that contribute to an effective increase in drag coefficient and treats them as a lumped percentage change in total drag acting over the interval $(h_{tr} \pm \Delta h_{tr})$ over which BLT can take place. Since drag changes are equivalent to density changes, the dispersion equations of Refs. 5 and 6 can be used to calculate this dispersion.

For the other part, the asymmetric aerodynamic moment of the rotating transition front will be considered for the worst case when its angular motion is such that this moment acts for an appreciable time in an inertial plane (the trajectory plane), i.e., when during a roll revolution of the body, the aerodynamic asymmetries are not canceled. This asymmetric aerodynamic contribution to dispersion is then treated analogous to the roll-through-zero case discussed in Section 5.4 of Ref. 6. It must be emphasized that this is a critical assumption that cannot now be established a priori. The validity is by inference from such sources as the flight-test data. Further discussion will follow below.

C. IMPACT DISPERSIONS DUE TO BOUNDARY LAYER TRANSITION

The analysis that follows assumes the altitude of transition, h_{tr} , to be the independent parameter.

Symmetric effects of boundary layer transition at h_{tr} are lumped into a drag increment $(\Delta C_D/C_D)_{tr}$. This increment is distributed linearly over an altitude $\pm \Delta h_{tr}$ above and below h_{tr} to approximate the temporal and spatial variabilities of the transition phenomenon. Above and below the $h_{tr} \pm \Delta h_{tr}$ interval, the transition-induced drag increment vanishes.

Aerodynamic asymmetries during boundary layer transition at h_{tr} are treated as a moment increment $\Delta C_{m_{tr}}$ about the center of gravity acting in a plane that remains space-fixed for a small but finite portion of the transition interval Δh_{tr} . This allows treating this case analogous to combining aerodynamic and geometric asymmetries with a roll-through-zero situation.

1. Symmetric BLT Effect on Dispersion

The approximate equations of Ref. 5 are used for rangewise impact dispersions resulting from deviations in density. The appropriate equation is:

$$\delta_{R_1} = \left(\frac{H}{V_E \sin \gamma_E} \right)^2 \frac{g}{\tan \gamma_E} I_5 \sum F_\rho \left(\frac{\Delta C_D}{C_D} \right)_{tr} \quad (1)$$

where

H = scale height of exponential atmosphere approximation, ft

V_E = reentry velocity, fps

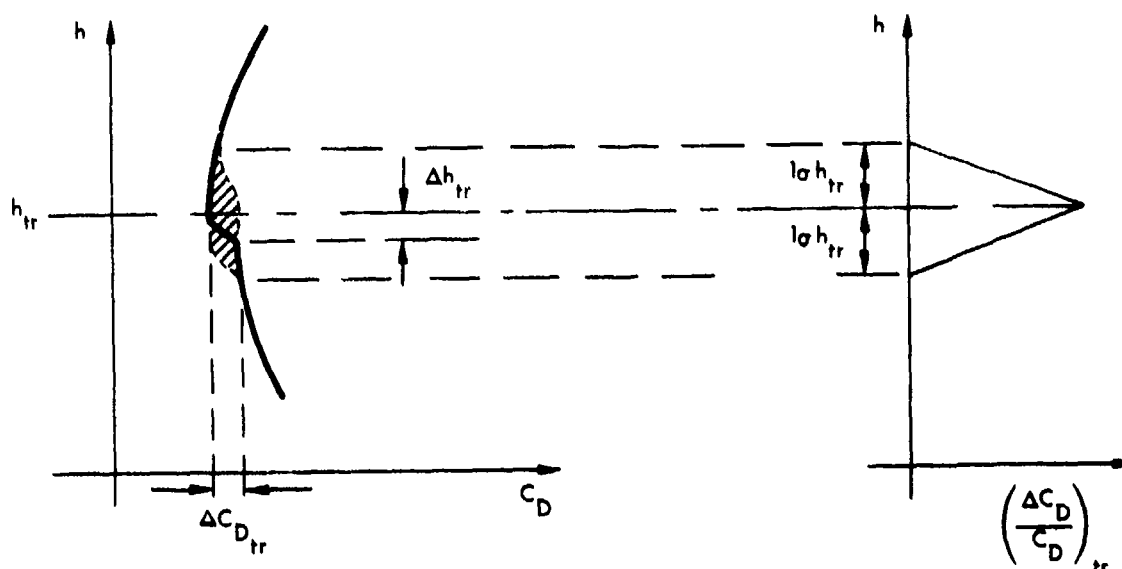
γ_E = reentry angle, deg

g = acceleration of gravity at sea level (SL)

I_5, F_ρ = functions of a parameter $K_{SL} = -P_{SL}/\beta \sin \gamma_E$ tabulated in Ref. 5; β = ballistic coefficient, psf;

P_{SL} = 2116 psf sea-level density

$(\Delta C_D/C_D)_{tr}$ = drag increment during boundary layer transition due to all symmetric effects, sketched in Fig. 3; this figure also sketches the assumed distribution of the $\Delta C_D/C_D$ variation over the $\pm 10h_{tr}$ band around the nominal altitude of transition h_{tr} .



12-8-75-7

FIGURE 3. Drag Increment During Boundary Layer Transition

Impact dispersions have been calculated from Eq. 1 for nominal transition altitudes from 100 kft to 20 kft, with a 1σ value of 6 percent of h_{tr} ,* for $(\Delta C_D/C_D)_{tr}$ of 0.1 and for ballistic coefficients of 1000, 2000, and 3000; reentry angles of 20, 30, and 50 deg; and reentry velocities of 16,000, 20,000, and 24,000 fps. A scale height H of 22,000 ft has been chosen to make the exponential atmosphere model the 30- to 100-kft altitude region.

Figure 4 shows the results as δ_{R1} versus h_{tr} for the three ballistic coefficients with δ_E and V_E as parameters.

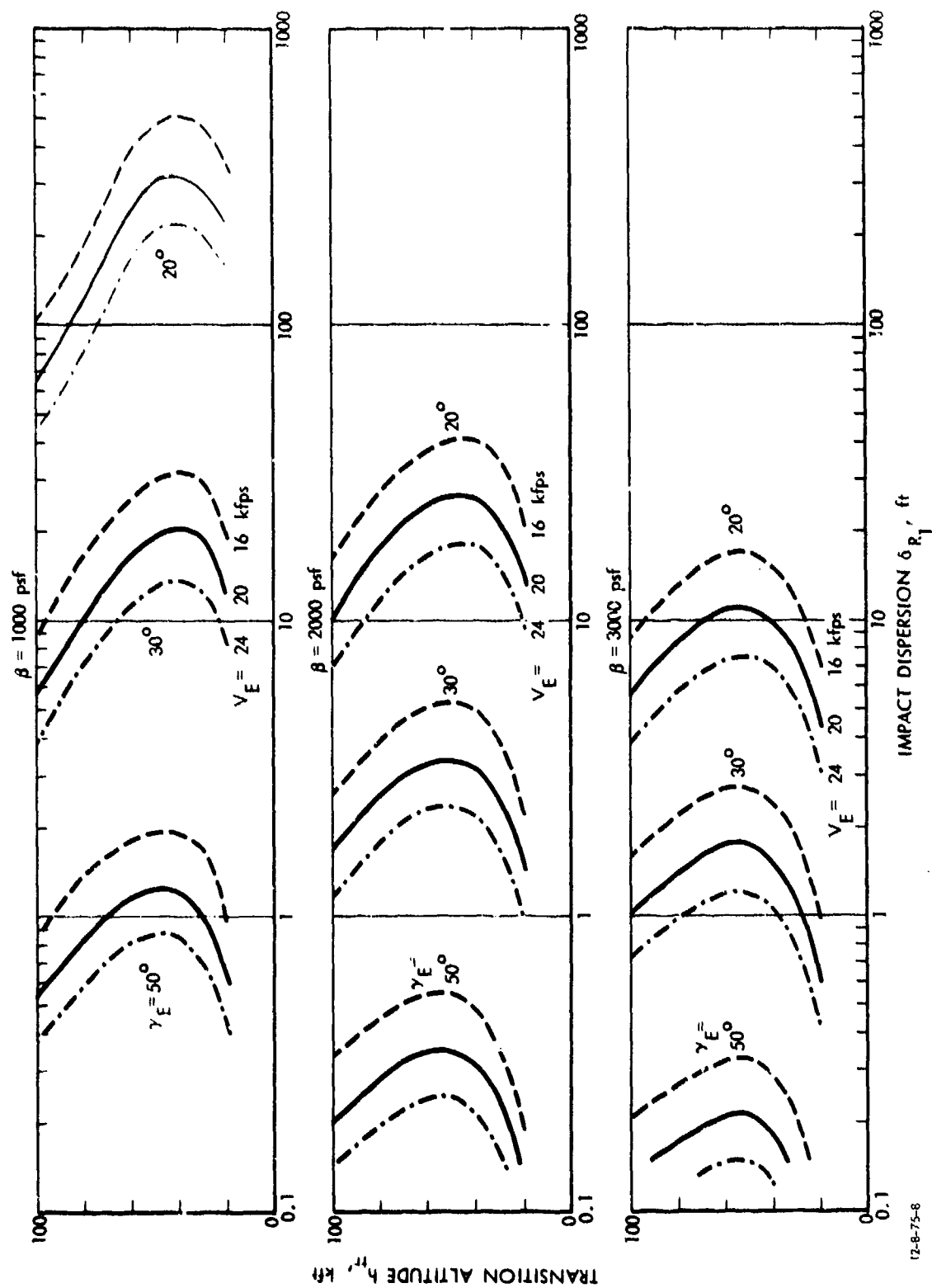
Except for the $\beta = 1000$ fps at 20 deg, the dispersions are about 100 ft or less with maxima around the 40,000-ft level. As expected, the dispersion decreases with steepening reentry angles and with increasing reentry velocities.

The $\delta_E = 20$ deg, $\beta = 1000$ data are shown by faint lines only with max dispersions around 1000 ft. These were considered too high, as the acceptable approximations of Eq. 1 are significantly exceeded (Refs. 5 and 6).

2. Asymmetric BLT Effects on Dispersions

Reference 6 develops equations for the effects on impact dispersions of aerodynamic and other asymmetries combined with constant and time-varying roll rates. The approach used in Section 5.4.2 of this reference for the special case of roll-through-zero is applied to our case of a BLT-induced aerodynamic asymmetric moment of a transient nature such that its plane of action remains fixed in the trajectory plane for a small, finite time. Figure 5 shows the situation at an instant when the plane of the transient BLT effect lies in the plane of the paper and is evidenced by a lift increment ΔL_{tr} acting at the

* A 1σ range of from 3 to 8 percent of h_{tr} seems indicated by flight data with multiple transition indicators and measuring instruments. For details see Ref. 7.



12-8-75-8

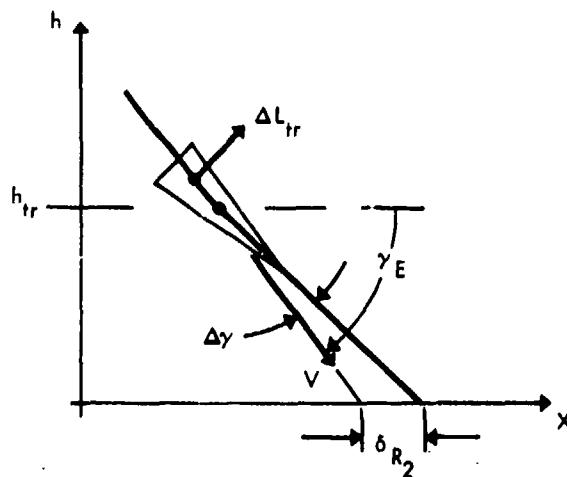
FIGURE 4. Impact Dispersions from Symmetric Boundary Layer Transition Effects
 $(\Delta C_D/C_D)_{tr} = 0.1$; $\Delta h_{tr}/h_{tr} = \pm 0.06$

center of pressure. With the usual simplifying assumptions of straight-line undisturbed flight paths ($\gamma = \gamma_E = \text{constant}$), it follows that the maximum rangewise effect on dispersion is

$$\delta_{R_2} = \frac{h_{tr} \Delta \gamma}{\sin^2 \gamma_E} \quad , \quad (2)$$

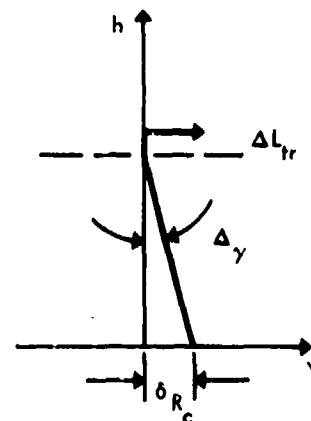
and in cross-range direction

$$|\delta_{R_C}| = \left| \frac{h_{tr} \Delta \gamma}{\sin \gamma_E} \right| = |\delta_{R_2} \sin \gamma_E| \quad . \quad (3)$$



12-8-75-9

(a) ΔL_{tr} in vertical plane



(b) ΔL_{tr} normal to vertical plane

FIGURE 5. BLT-Induced Effects on Trajectory

The incremental change in path angle $\Delta\gamma$ is given by

$$\Delta\gamma = \int_{t_{tr \text{ onset}}}^{t_{tr \text{ completion}}} \dot{\gamma} dt \sim \frac{\delta\gamma}{\delta t} \Delta t_{tr} \quad (4)$$

The time interval Δt_{tr} can be related to the altitude interval

$$\Delta h_{tr} = \Delta t_{tr} V \sin\gamma_E \quad (5)$$

However, only a fraction "a" of the time of transition is assumed to be acting in a space-fixed plane, so that

$$\Delta t_{tr} = a \frac{\Delta h_{tr}}{V \sin\gamma_E} \quad (6)$$

Neglecting gravity and centrifugal force terms, the acceleration normal to the path can be written as $V \frac{\delta\gamma}{\delta t}$; hence

$$\frac{\delta\gamma}{\delta t} = \frac{\Delta L_{tr} g}{WV} \quad (7)$$

and substituting Eqs. 6 and 7 into Eq. 4 gives

$$\Delta\gamma = \frac{\Delta L_{tr} g}{WV^2 \sin\gamma_E} a \Delta h_{tr} \quad (8)$$

The incremental lift ΔL_{tr} can be related to the BLT-induced aerodynamic moment increment $\Delta C_{m_{tr}}$ and other basic aerodynamic and geometric characteristics of the vehicle (see Fig. 6) as follows:

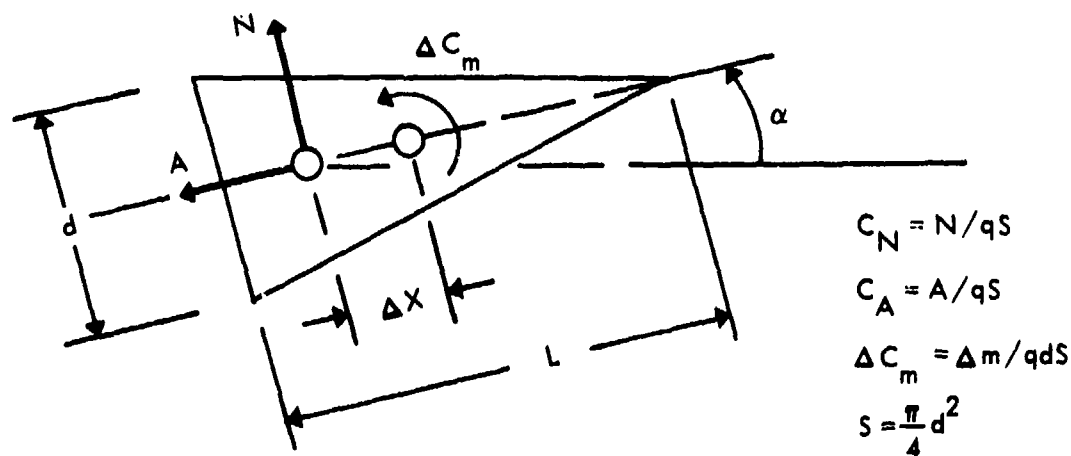
$$\begin{aligned}
 \Delta L_{tr} &= C_{L\alpha} \alpha_{tr} qS \\
 &= (C_{N\alpha} - C_A) \frac{\Delta C_{m_{tr}}}{C_{N\alpha} \frac{\Delta X}{d}} \frac{\rho V^2}{2} S \\
 &= \frac{\left(1 - \frac{C_A}{C_N}\right) \rho V^2 S}{2 \left(\frac{\Delta X}{L}\right) \left(\frac{L}{d}\right)} \Delta C_{m_{tr}}
 \end{aligned} \tag{9}$$

where

C_A = the axial (\approx drag) force coefficient

$C_{N\alpha}$ = the normal force coefficient slope

$\Delta X/L$ = the static margin.



12-8-75-10

FIGURE 6. Geometric and Aerodynamic Relations

Combining Eqs. 8 and 9 with Eq. 2 gives

$$\delta_{R_2} = \frac{\rho g}{2} \frac{S}{W \sin^3 \gamma_E} \frac{\left(1 - \frac{C_A}{C_{Na}}\right)}{\left(\frac{\Delta X}{L}\right) \left(\frac{L}{D}\right)} a h_{tr} \Delta h_{tr} \Delta C_{m_{tr}} . \quad (10)$$

This relation can be rearranged and simplified by introducing the ballistic coefficient β for the $\frac{S}{W}$ term

$$\beta = \frac{W}{C_A S} , \quad (11)$$

and approximating the density by an exponential approximation

$$\rho = \rho'_0 e^{-h_{tr}/H} , \quad (12)$$

where

H = scale height

ρ'_0 = extrapolated sea-level value of ρ corresponding to value of H selected for best match of ρ over an altitude region of interest. In subsequent calculations $H = 22,000$ to favor the 30- to 100-kft region, and $\rho'_0 = 0.00322$ slug/ft³ (1962 standard atmosphere).

In addition, the altitude interval of transition Δh_{tr} can be approximated as a fraction "b" of altitude of transition itself, or

$$\Delta h_{tr} = b h_{tr} . \quad (13)$$

With the last three expressions, then, Eq. 10 for the impact dispersion δ_{R_2} becomes

$$\delta_{R_2} = \frac{g\rho_0}{2} \frac{ab\left(\frac{1}{C_A} - \frac{1}{C_{Na}}\right)}{\left(\frac{\Delta X}{L}\right)\left(\frac{L}{D}\right)} \frac{\Delta C_{m_{tr}} h_{tr}^2 e^{-h_{tr}/H}}{\beta \sin^3 \gamma_E} \quad (14)$$

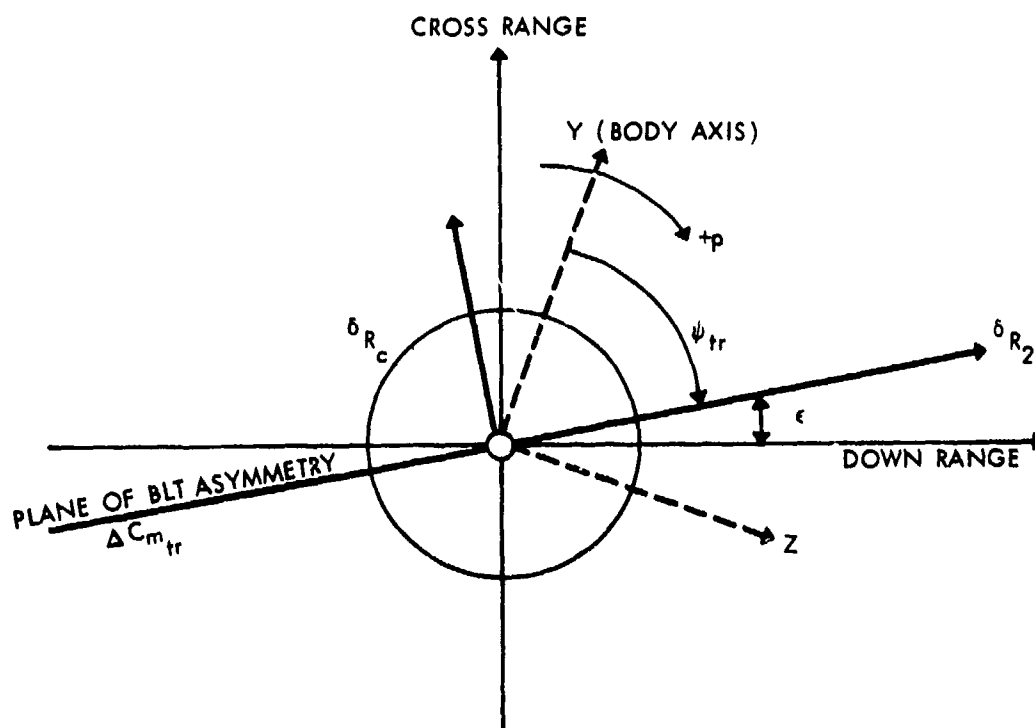
It is noted that the reentry angle is the most powerful parameter as lofting (increasing γ_E) reduces δ_{R_2} through the $\sin^3 \gamma_E$ term. The reentry angle effect in this case is greater by a factor $1/\cos \gamma_E$ over the lumped drag increment case of δ_{R_1} given previously in Eq. 1. Increases in β and static margin decrease δ_{R_2} only linearly; δ_{R_2} is, of course, directly proportional to the magnitude and sense of the asymmetric aerodynamic perturbing moment $\Delta C_{m_{tr}}$, and the fractions a and b correspond, respectively, to the fraction of transition time over which $\Delta C_{m_{tr}}$ acts in a space-fixed plane and to the fraction of transition altitude devoted to the transition process. Note that the reentry velocity has disappeared from this expression.

Partial differentiation of Eq. 14 shows that if h_{tr} is the only variable, the impact dispersion is maximum at $h_{tr} = 2H$ and approaches zero as $h_{tr} \rightarrow 0$ and $h_{tr} \rightarrow \infty$ (i.e., greater than about 200 kft). Furthermore, the δ_{R_2} curve has points of inflection, at $h_{tr_1} = 3.414H$ and $h_{tr_2} = 0.586H$. Similarly, large betas ($\beta \rightarrow \infty$) and very steep reentry angles ($\gamma_E \rightarrow 90$ deg) minimize the dispersion, as expected.

The analysis so far has assumed that the plane of the BLT-induced aerodynamic asymmetry $\Delta C_{m_{tr}}$ acts in the plane of the trajectory. A reentry vehicle, rolling about its longitudinal axis with a roll rate p , experiences this particular case only when the circumferential rate of rotation of the BLT asymmetry is roughly equal to, but opposite to, the roll rate, and if the onset of the asymmetry occurs while its plane of action is nearly

aligned with the trajectory plane. Thus, Eq. 14 for δ_{R_2} represents the worst case of impact dispersion due to $\Delta C_{m_{tr}}$. The more general case is sketched in Fig. 7, which shows the base of a rolling reentry vehicle, for simplicity, descending vertically ($\gamma_E = 90$ deg), with a BLT asymmetry $\Delta C_{m_{tr}}$ at a (time-varying) angle ψ_{tr} relative to body-fixed axis. With $d\psi_{tr}/dt$ equal and opposite to the roll rate p , the angle ϵ between the asymmetry and the trajectory plane remains constant. The resultant up- or down-range impact dispersion is then

$$\begin{aligned}\delta_R &= \pm(\delta_{R_2} \cos \epsilon - \delta_{R_C} \sin \epsilon) \\ \delta_C &= (\delta_{R_2} \sin \epsilon + \delta_{R_C} \cos \epsilon)\end{aligned}\quad (15)$$



12-8-75-11

FIGURE 7. Trajectory-Asymmetry-Body Axes Relations

Equations 14 and 3, then, represent the maximum impact dispersions only for $\epsilon \approx 0$ and $d\psi_{tr}/dt = -p$. For $\epsilon = \text{constant} \neq 0$, Eqs. 15 apply and for the most general case when $\epsilon = \epsilon(t)$, a time-varying impact dispersion can be obtained from these equations. Subsequent analyses will concentrate on the worst case given by Eqs. 14 and 3.

Calculations for this component of impact dispersion have been made for the same range of nominal transition altitudes of from 150 to 10 kft; ballistic coefficients of 800, 1000, 1500, 2000, 2500, and 3000; and reentry angles from 10 to 70 deg.

For slender sphere-cones the aerodynamic coefficient term $(1/C_A - 1/C_{N\alpha})/(\Delta X/L)(L/D)$ reduces to roughly 100 for a static margin $(\Delta X/L)$ of 3.5 percent, 50 for 7 percent $(\Delta X/L)$ and 25 for 14 percent $(\Delta X/L)$. The 7 percent static margin case has been calculated.

Typical values of the incremental moment coefficient can be taken from Refs. 8, 9, and 10. The flight-derived data of Ref. 8 indicate a $\Delta C_{m_{tr}} \sim -0.0003$ to -0.002 ; wind tunnel data from Ref. 10 give -0.001 to -0.03 , and from Ref. 9, -0.001 to -0.003 . This large spread of magnitude is not unexpected, and will be one of the major uncertainties for some time to come. A value of -0.001 has been used in the calculations.

The transition altitude interval seems to be between 0.1 and 0.2 of h_{tr} . A value of $b = (\Delta h_{tr}/h_{tr}) = 0.10$ has been chosen for the sample calculations. It is recognized that this may be too low a value for the higher altitude regimes of transition onset and for heat shields that are rough or of low-temperature ablative materials. For low transition altitudes, when the likelihood of rapid flashing forward of BLT is high, the fraction b could well be much smaller than 0.1. The fraction a has been chosen as $a = 0.5$, corresponding to the case when the asymmetric BLT moment remains in the down-range plane for

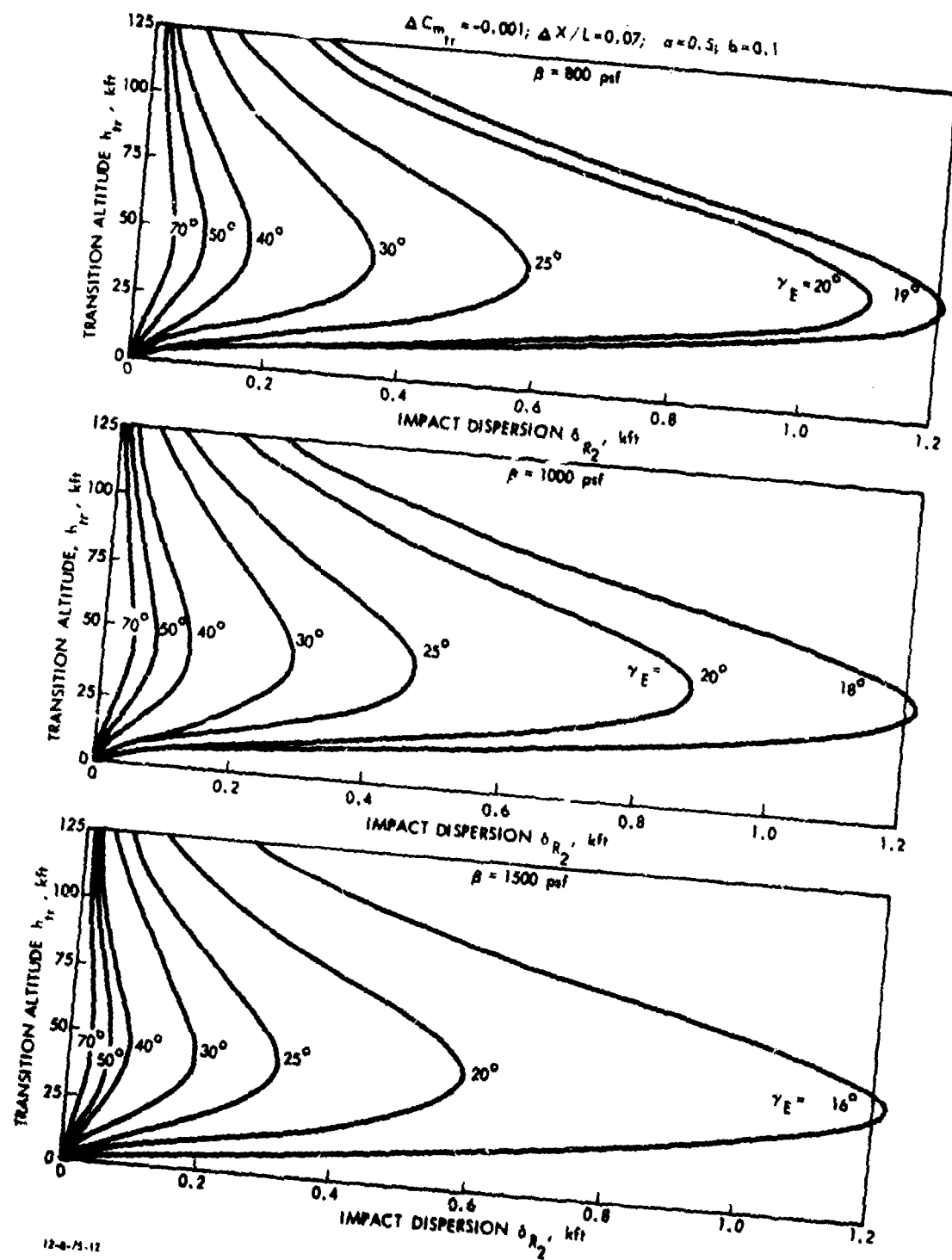
half the BLT transition period.* For example, at $V = 20,000$ fps, $\gamma_E = 22$ deg, $b = 0.1$, $h_{tr} = 100$ kft, Eq. 6 gives $\Delta t_{tr} = 0.67$ sec for the BLT period.

Figures 8 and 9 show the results for this asymmetric BLT effect on impact dispersions. For values of $\Delta C_{m_{tr}}$, $(\Delta X/L)$, a , b different from those selected for these calculations, Table 1 lists the scale factors to be applied to the δ_{R_2} values of these figures.

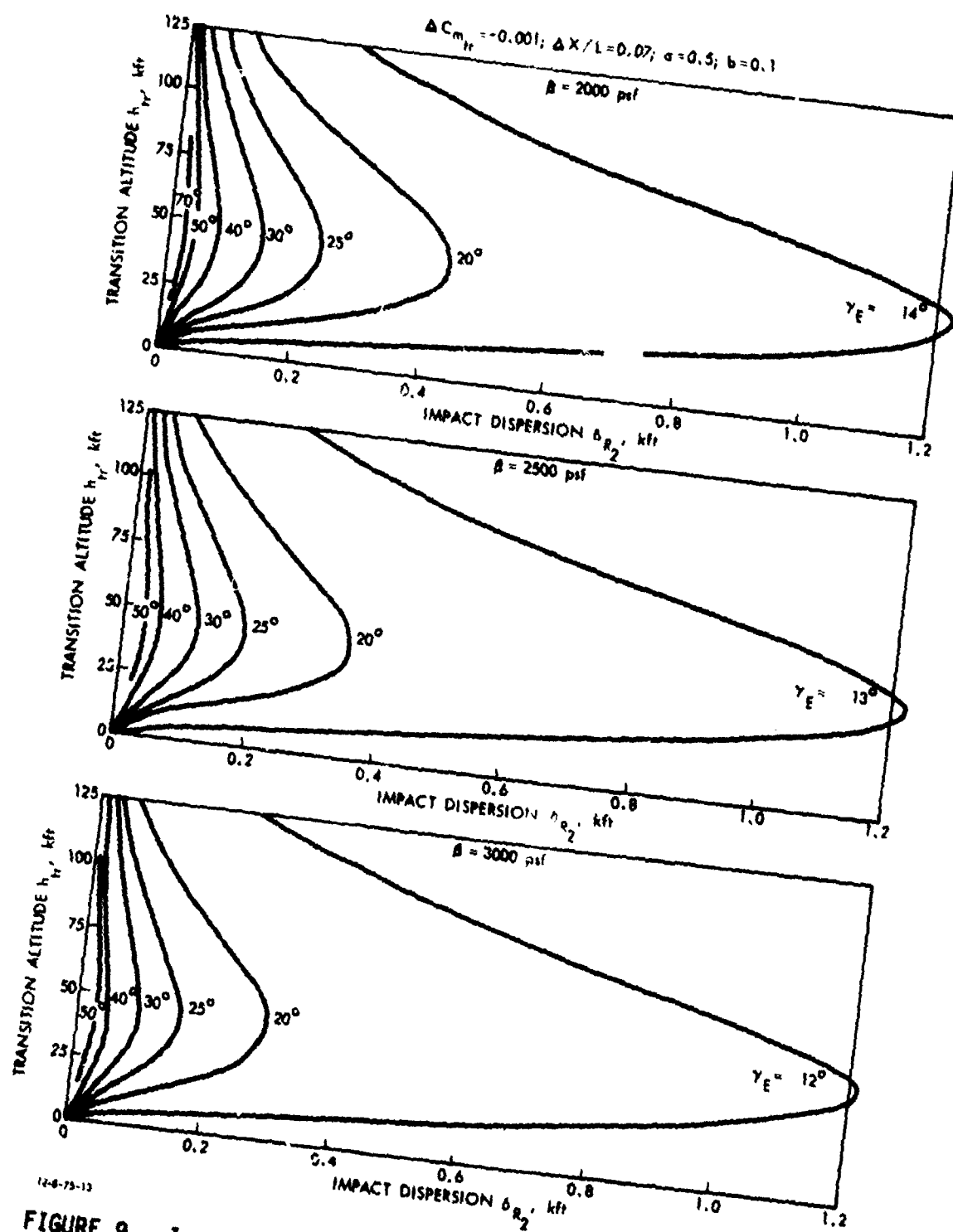
Considering the range of the aerodynamic moment increments given in Refs. 8, 9, and 10, a $\Delta C_{m_{tr}} = 0.01$ gives ten times larger δ_{R_2} than given in Figs. 8 and 9, and a $\Delta C_{m_{tr}} = 0.03$ would give 30 times larger values. No matter what alleviating values for a , b , and static margin may be used, these δ_{R_2} values are very, very large for these large moment increments, even for high ballistic coefficient vehicles at steep reentry angles. Hence, every effort must be made to keep $\Delta C_{m_{tr}}$ as small as possible.

Unfortunately, we have neither theoretical guidance nor adequate empirical data as to what design parameters, materials characteristics, and dynamic effects could accomplish this, and how $\Delta C_{m_{tr}}$ might vary with altitude. Similarly unknown are the design, materials, and dynamic impacts on the magnitudes of parameters a and b and their dependence on altitude so that positive steps may be taken to keep them as small as possible for the region of transition altitude to be expected.

As mentioned previously, this is an assumption that cannot presently be supported experimentally or theoretically. It is the author's judgment of a worst case based on the further assumption that there exists a cause-effect relation between the rotation of the BLT region, the RV rotation dynamics, and the properties of the materials. Clearly these are critical assumptions that need further study.



12-8-75-12
FIGURE 8. Impact Dispersions from Asymmetric Boundary Layer Transition Effects



12-8-75-13
 FIGURE 9. Impact Dispersions from Asymmetric Boundary Layer Transition Effects

TABLE 1. SCALE FACTORS FOR IMPACT DISPERSIONS GIVEN IN FIGURES

<u>PARAMETER</u>	<u>SYMBOL</u>	<u>MULTIPLY δ_{R_2} BY</u>
Aerodynamic Moment Increment	$\Delta C_{m_{tr}}$	$\frac{\Delta C_{m_{tr}}}{0.001}$
Static Margin	$\frac{\Delta X}{L}$ in %	$\frac{7.0}{(\Delta X/L)_\%$
Ratio $\frac{\text{Transition Interval}}{\text{Altitude of Transition}}$	b	$\frac{b}{0.10}$
Fraction of $\Delta C_{m_{tr}}$ in Space-Fixed Plane	a	$\frac{a}{0.50}$
Scale Height H	$\left\{ \begin{array}{l} H, h_{tr} \text{ in kft} \\ \rho_0 \text{ in } \frac{\text{slugs}}{\text{ft}^3} \end{array} \right.$	$\frac{\rho_0 e^{-h_{tr}/H}}{0.00333 e^{-h_{tr}/22}}$

D. DISCUSSION

Both symmetric and asymmetric effects of boundary layer transition maximize impact dispersions if transition occurs around the 40- to 50-kft altitude region. Above and below this altitude region, both components of dispersion decrease toward zero at sea level and at very high altitudes. However, the symmetric component is very much smaller than the asymmetric one and is of a magnitude generally included in traditional analyses of dispersions due to uncertainties in drag or ballistic coefficients. Hence, only the asymmetric component of the dispersion will be discussed in detail.

The analogy to the roll-through-zero problem of the transition-induced aerodynamic asymmetries and their impact dispersions has been noted earlier. The results of Figs. 8 and 9 indicate that the magnitude of the dispersions can be as severe as in roll-through-zero cases. The probability of occurrence of this worst case may or may not be similar to the roll-through-zero probability, but it seems prudent to investigate what could be done to keep the worst dispersion as small as possible, just as it is desirable to avoid a roll-through-zero condition altogether. The major parameters affecting dispersion are discussed in order of their relative importance, namely, reentry angle γ_E , asymmetric moment coefficient $\Delta C_{m_{tr}}$ and the fraction a of the transition interval when its plane of action coincides with the trajectory plane, ballistic coefficient β , static margin, and fraction b of nominal transition altitude over which actual transition takes place.

1. Reentry Angle γ_E

The reentry angle is the most powerful parameter available, as an increase in γ_E reduces impact dispersion as $1/\sin^3 \gamma_E$, regardless of nominal altitude of transition. However, steepening the reentry path increases heating rates, shear stresses, stagnation pressures, and deceleration loads. Hence, if boost energy is available for lofting the trajectory, the maximum feasible reentry angle may be set more by the limits of the heat shield and tip materials to absorb the more severe environment in a safe and shape-stable manner than by an impact dispersion limit.

2. Asymmetric Moment Coefficient $\Delta C_{m_{tr}}$ and Fraction a

These are by far the most difficult parameters to assess and bound, for two reasons. First, only very limited data have been extracted from test data and, second, the concept of a transition front rotating around a body has apparently not been studied. There are three specific characteristics of $\Delta C_{m_{tr}}$ one

needs to know, namely its magnitude, its rate of circumferential rotation, and how these two vary with altitude.

The aerodynamic asymmetry could also be given in terms of a BLT-related trim angle of attack $\Delta\alpha_{tr}$ in accordance with Eq. 16.

$$\Delta C_{m_{tr}} = C_{N\alpha} \Delta\alpha_{tr} (AX/L)(L/d) \quad (16)$$

For a 7 percent static margin slender sphere-cone, the corresponding $\Delta C_{m_{tr}}$ and $\Delta\alpha_{tr}$ values are roughly

$\Delta C_{m_{tr}}$	0.0001	0.001	0.01
$\Delta\alpha_{tr}$	0.015 deg	0.15 deg	1.5 deg

As to the magnitude, the wind tunnel and flight results of Refs. 8, 9, and 19 indicate several orders of magnitude, but even within each set of data, an order of magnitude or more can be observed. Even with an order of magnitude increase in $\Delta C_{m_{tr}} = 0.001$ (used in Figs. 8 and 9), the resulting worst-case impact dispersions seem unacceptably high. Hence, knowledge of the magnitude, ability to predict its values, and ultimately a capability to minimize its magnitude are pressing goals for this technology.

Regarding the circumferential rotation, only Ref. 8 has some results, but not in a format that would allow assessing the probability of the plane of action of $\Delta C_{m_{tr}}$ remaining in the trajectory or any other space-fixed plane. This is an important aspect, as it is quite possible that the coincidence of the $\Delta C_{m_{tr}}$ plane with a space-fixed plane could happen more than once, in contrast to the roll-through-zero case where there is only one instant (roll rate = 0) when any trim lift is not canceled and can bend the trajectory. The data reduction and analysis techniques used in Ref. 8 could probably be extended

to provide the angular rates of rotation of the $\Delta C_{m_{tr}}$ plane for properly instrumented vehicles. Only after a meaningful set of such rotational rate data has been assembled, from as many RVs as possible, can one determine if the use of the parameter a^* is adequate to determine the fraction of the transition period during which the $\Delta C_{m_{tr}}$ plane remains space-fixed.

Finally, the variation with altitude of transition of both magnitude and plane of action of $\Delta C_{m_{tr}}$, and space-fixed period for fraction a , must be determined. Altitude regions below 25 kft and above 100 kft are of interest as they avoid the dispersion maxima of the 40- to 50-kft band.

Even if one were able to choose a transition altitude to minimize the dispersions discussed here, there are several other performance characteristics affected by the altitude of transition. These collateral effects are pointed out in paragraph 5 below.

It is obvious that both magnitude and orientation of $\Delta C_{m_{tr}}$, and their variation with altitude, are dependent on the many interrelated and interacting parameters of the boundary layer transition process. Thus all our theoretical and empirical shortcomings of understanding and predicting transition directly affect our likelihood of bounding $\Delta C_{m_{tr}}$. An empirical correlative approach may be our only means of progress for some time to come.

3. Ballistic Coefficient and Static Margin

Increasing the ballistic coefficient and the static margin decrease impact dispersion proportionally. Their values, however, will probably be set by other design and performance requirements. There is, of course, a possible interplay between the static margin and $\Delta C_{m_{tr}}$ that needs to be watched for as data on $\Delta C_{m_{tr}}$ are accumulated.

* Note the footnote on page 20.

4. Fraction b

This parameter should also be dependent on the complex process of transition. Conceptually one would expect b to be larger at higher altitudes than at lower ones. The lower Reynolds numbers at higher altitudes give rise to more stable boundary layers that can resist disturbances tending to cause turbulent spots, especially at hypersonic speeds. Hence, transition should take more time or altitude to go from onset to completion. Whether this is strong enough to increase b at high altitudes remains to be determined from a careful analysis of test data from appropriately instrumented vehicles.

5. Collateral Effects of Altitude of Transition

It has been pointed out that a significant reduction of the transition-related impact dispersions can be realized if the actual altitude of transition is as far as possible above or below the 40- to 50-kft altitude region. The preponderance of transition altitudes occurring above 50 kft seems to have led many to dismiss the possibility of low altitudes of transition. Fortunately, the SAMAST series (Ref. 7) of flights has shown that low transition altitudes can be achieved and repeated. The basic reason for not dismissing the low-altitude option is that high transition altitudes can get us into severe problems of survival, dispersion, and wake signature. Specifically, high altitudes of transition lead to long periods of turbulent heating. This means major increases in heat pulse, tip and heat shield recessions, and tip-shape asymmetries and changes. An extended period of turbulent boundary layer flow is capable of generating large-scale macroscale roughness that locally amplifies the already high turbulent heat transfer by factors from 2 to 4, thereby enhancing rapid shape changes and local asymmetries. Furthermore, the electromagnetic characteristics of the wake from a reentry vehicle with fully turbulent flow beginning at higher altitudes cause a significant increase and change in radar signature. Hence, if it were feasible to raise

the altitude of transition significantly to keep the BLT-induced dispersions small, one would have to trade this gain against the penalties on survival, dispersion, and penetrability caused by the extended period of turbulent flow conditions.

Beside the above considerations of RV performance, there is a fundamental question of fluid mechanics as to how high one could raise the altitude of transition under hypersonic, low Reynolds number conditions or to how low an altitude one could maintain laminar flow (below what SAMAST vehicles have achieved). The current state of basic knowledge of the transition phenomenon under these conditions does not appear adequate to tell us today how to do either except by extensive experimentation. A systematic theoretical and experimental research effort would be helpful to develop an understanding and guidance for future choices of optimum altitudes of transition.

One can conclude this discussion by noting that all parameters (except reentry angle, ballistic coefficient, and static margin) that affect impact dispersions due to asymmetric boundary layer transition effects are directly related to the phenomenon and the uncertainties of the transition process itself. The topic of asymmetric effects must, therefore, be added to our current efforts of understanding tip-shape changes, material properties, and ablative performance in the context of the boundary layer transition phenomenon. This will involve mostly empirical correlations of carefully selected and processed test data, but should be supplemented by a concurrent analytic theoretical attack on the question of what might be the basic forcing functions for the circumferential motion of an asymmetric transition front. Without such effort we will not know how to keep this dispersion component under control except through trajectory shaping and we will be at the mercy of the statistics of occurrence and severity of the asymmetric effects.

III. IMPACT DISPERSION ESTIMATES

A. BACKGROUND

This section collects representative values for various contributors to ballistic reentry vehicle dispersions so that the relative importance of each component may be assessed. Only RV related dispersions are considered over a range of reentry angles from 20 to 60 deg, reentry velocities from 16,000 fps to 24,000 fps, and for ballistic coefficients from 1000 to 3000 psf. Readily available results or simple approximate equations were used in this relative quantitative assessment. Three dispersion components are considered. The first is the conventional one that includes wind, density, and symmetric drag uncertainties. Second, a component due to roll-trim dynamics including roll-through-zero is treated. Boundary layer transition effects on dispersions, the third component, are taken from Section II. A separate section is devoted to each component, describing the assumptions made and presenting the results in graphical format. Finally, the magnitude of the components that are poorly understood today is referenced to the conventional component, which is pretty well understood in cause and magnitude. This relative comparison highlights the complex interacting effects of ballistic coefficient, reentry angle, and velocity. As neither the magnitudes nor the proper statistical treatment of the non-conventional components is known to any degree of engineering adequacy, their ratios to the well-known component will indicate the degree of urgency in developing the technology base for better understanding and quantitative estimation of these uncertain components of dispersion.

B. CONVENTIONAL DISPERSION COMPONENTS

The effects of wind, density, and drag variations during reentry are generally considered as conventional dispersion contributors. Included in the drag variation are the combined effects during reentry of symmetrical nose-shape changes, of Mach number changes from free molecule to continuum flow regimes, of weight changes, of trim angles of attack, as well as of the initial angle of attack at reentry. A 3 percent total, symmetrical, drag coefficient uncertainty is a reasonable bound for an RV which has been through a full R&D, DASO and OT sequence of instrumented test phases. Reference 5 gives approximate results for rangewise dispersions for a 10 percent drag deviation. These results have been scaled down to the 3 percent ($\Delta C_D/C_D$) values assumed for our calculations.

Wind and density contributions have been taken from Ref. 11, which calculated these terms from 2σ deviations from the January mean profile of 60 deg N latitude.

It is recognized that we have today the capability of working with weekly if not daily weather statistics throughout the year over specific geographic sectors. Such a modern statistical data base of shorter spans would be likely to lower the dispersion contributions based on a January monthly base. However, no readily available dispersion data of such finer statistical mesh were available, hence the results of Ref. 11 have been used without modifications.

The dispersion contributions from 3 percent drag and 2σ deviations from a January mean in wind and density have been root-sum-squared (RSSd) to arrive at a single conventional range-wise impact dispersion δ_{RSS} as a function of reentry angle and ballistic coefficient. The results are shown in Fig. 10 for three ballistic coefficients at a reentry velocity of 20,000 fps. The modest effects of other reentry velocities, namely 16,000 and 24,000 fps, are indicated as well as the proportionate

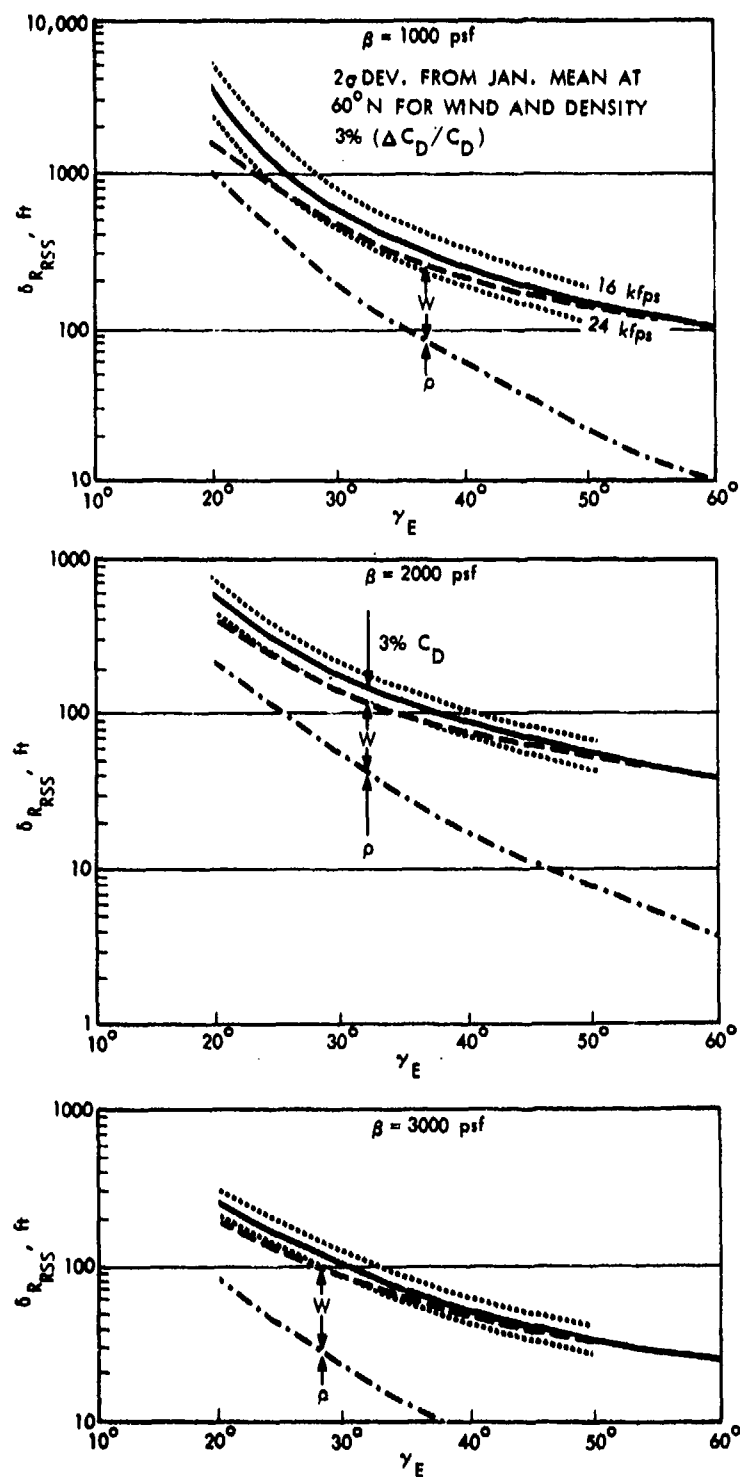


FIGURE 10. Rangewise Dispersions Due to RSSd Wind-Density and Drag Contributions Versus γ_E for Three β s at $V_E = 20$ kfps

contributions of density (ρ), wind (w), and 3 percent drag. As attention in this analysis is focused on the larger, rangewise component of dispersion, the cross-range contributions of a crosswind and an initial angle of attack dynamic effect are not estimated.

C. ROLL-DYNAMICS DISPERSION COMPONENTS

Asymmetric shape changes during reentry, especially on the nose tip, lead to trim angles of attack which, when combined with center of gravity offsets and/or mass asymmetries, lead to roll-dynamics effects contributing to dispersion components in both rangewise and cross-range directions.

Under certain conditions the roll rate may change so that it becomes nearly the same as the aerodynamic pitch-yaw frequency. This represents the "lock-in" or roll resonance case, which amplifies the angle of attack and leads to some dispersion. Most severe, however, is the case when aerodynamic roll torque and/or trim-center-of-gravity offset conditions are such as to cause the roll rate of the vehicle to go through zero. In this roll-through-zero (RTZ) case the trim lift is not canceled as the RV stops rolling a small but finite instant causing the trajectory to bend, which propagates into an impact dispersion of extreme magnitude.

Reference 6 discusses the roll dynamics, both the roll resonance and the roll-through-zero case, in great detail and derives approximate equations for the magnitudes of these dispersion contributions. For our purposes, the following conclusions are significant:

- Impact from roll dynamics can be anywhere on an ellipse with its semi-major axis along the trajectory and having a magnitude between zero and the maximum calculated as the worst case.

- The ratio of minor to major axis of the impact ellipse is $|\sin \gamma_E|$.
- The usual assumptions of combining dispersion components as independent, normally distributed ones are not generally appropriate to the roll-dynamics cases.
For the roll-through-zero case, one must determine the probability of encountering or exceeding a given value of the rangewise dispersion for given trim angles of attack; this combines the probability of encountering zero roll rate with the probability of encountering a given magnitude of dispersion for the semi-major axis.
- Dispersions from simple roll resonance are at least an order of magnitude smaller than those from roll-through-zero.
- In view of the last conclusion, only the roll-through-zero case will be analyzed. The maximum or worst case rangewise dispersion is calculated from the equation in Ref. 6 in the following form:

$$\delta_{R_{RTZ}} = 1.49 \left(\frac{C_{N\alpha}}{C_A} - 1 \right) \sqrt{\frac{P_{SL}}{H}} \frac{1}{\sqrt{P_E}} \left(\sqrt{\frac{V_E}{B}} \frac{1}{\sin^2 \gamma_E} \right) E \bar{\alpha}_0 \quad (17)$$

where

- 1.49 = dimensionless constant
- $C_{N\alpha}$ = normal force coefficient slope
- C_A = axial (~drag) force coefficient
- P_{SL} = sea-level pressure (2116 psf)
- H = scale height for exponential atmosphere, ft
- P_E = initial roll rate at reentry, rad/sec
- V_E, γ_E = reentry velocity (ft/sec) and angle (deg)
- E = (ft), function of altitude of roll-through-zero, atmosphere, ballistic coefficient, and reentry angle (see Fig. 5.3 of Ref. 6)
- $\bar{\alpha}_0$ = trim angle due to asymmetries, radians

Values of $\delta_{R_{RTZ}}$ have been calculated from this equation for zero-roll-rate altitudes of about 25 kft (where E is a maximum for the β s and γ_E s of interest) and at 100 kft. For the remaining parameters the following values were used:

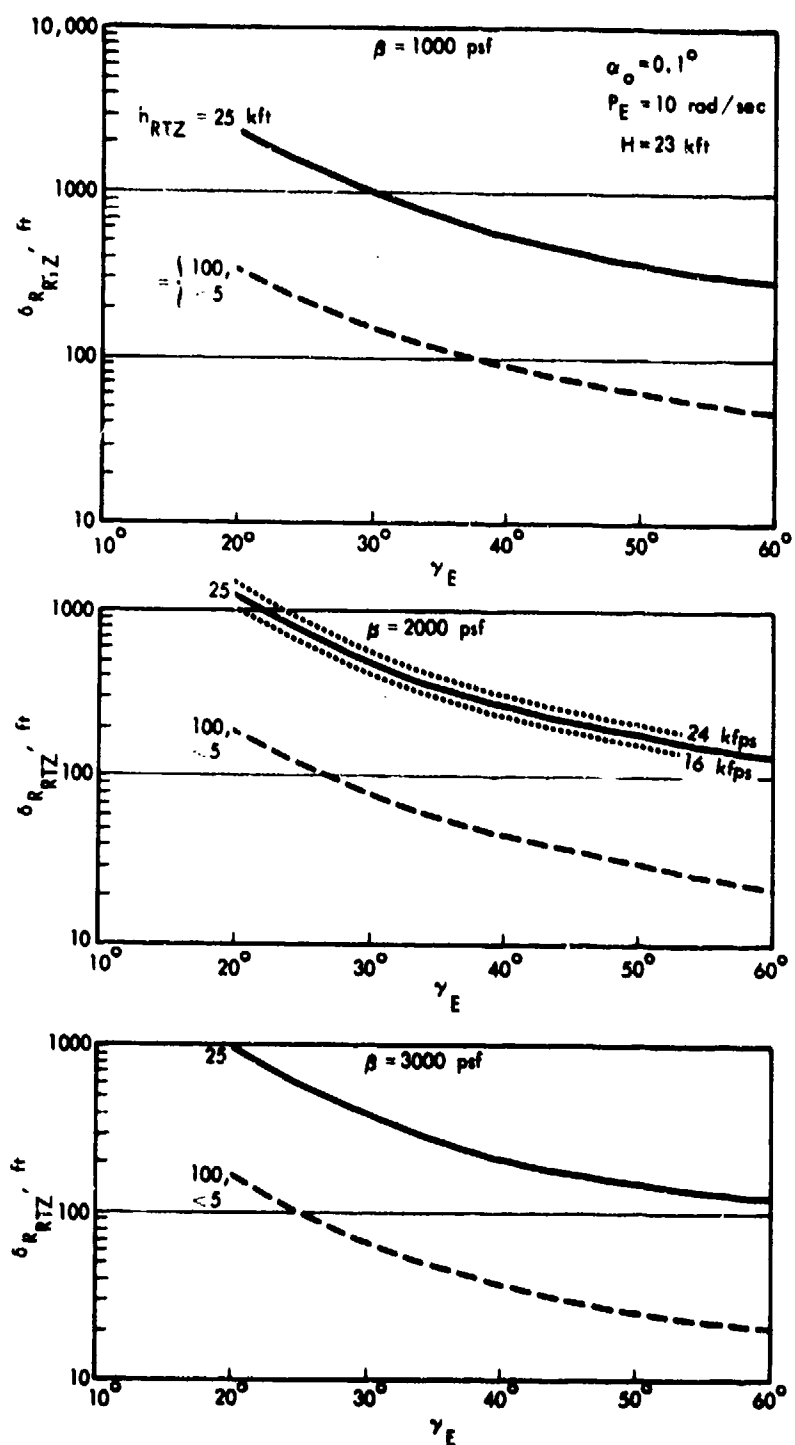
$$\begin{aligned}\bar{\alpha}_0 &= 0.1 \text{ deg} \\ p_E &= 10 \text{ rad/sec} \\ (C_{N\alpha}/C_A - 1) &= 20 \\ \sqrt{P_{SL}/H} &= 0.3 \text{ (or } H \sim 22 \text{ kft)} \\ V_E &= 16, 20, 24 \text{ kfps} \\ \gamma_E &= 20, 30, 40, 50, 60 \text{ deg} \\ \beta &= 1000, 2000, 300 \text{ psf.}\end{aligned}$$

The results are summarized in Fig. 11 showing $\delta_{R_{RTZ}}$ maximum versus the reentry angle for the three ballistic coefficients. The maximum dispersions occur when the roll rate goes through zero near 25 kft. For zero roll at 100 kft or at less than 5 kft (because of the behavior of function E), the dispersions are significantly less and are also shown in Fig. 11. The effect of changing reentry velocity from 20 to 16 or 24 kfps is indicated on the $\beta = 2000$ curve.

The actual rangewise dispersions for this component can then be any value between zero and the maxima shown, depending on the probability of encountering or exceeding this particular value at a trim angle of $\bar{\alpha}_0 = 0.1$ deg. For other trim values, or initial roll rate p_E other than 10 rad/sec, Eq. 17 indicates how the results can be scaled.

From the magnitude of the rangewise dispersion, and remembering that the cross-range dispersion is $\sin \gamma_E$ times $\delta_{R_{RTZ}}$, it is clear that every effort has to be made to prevent roll-through-zero from occurring.

Since it appears, from the results of Ref. 6, that the roll resonance situation gives dispersions at least an order of magnitude lower than those calculated for roll-through-zero, it is



12-6-75-15

FIGURE 11. Maximum Rangewise Dispersion Due to Roll-Through-Zero at Several Altitudes Versus γ_E for Three β s at $V_E = 20$ kfps

clear that aerodynamic asymmetries must show at least one or more degrees trim under lock-in conditions in order to cause comparable dispersions.

D. BOUNDARY LAYER TRANSITION DISPERSION COMPONENTS

The dispersion components due to boundary layer transition effects were discussed in detail in the preceding Section II. The results of the approximations derived therein are taken directly from Fig. 4 for the symmetric component and from Figs. 8 and 9 for the asymmetric one. They are presented as maximum rangewise dispersions $\delta_{R_{BLT}}$ versus reentry angle for three ballistic coefficients for transition altitudes of around 45 kft (where $\delta_{R_{BLT}}$ is maximum) and at 100 kft (and 15 kft or less where $\delta_{R_{BLT}}$ equals the value at $h_{tr} = 100$ kft). Both the symmetric component δ_{R_1} for $V_E = 20$ kfps and the much larger asymmetric one, δ_{R_2} , are shown in Fig. 12.

It might be well to recap the values of the input parameters used in Section II for the two BLT dispersion components. The symmetrical component δ_{R_1} was calculated from Eq. 1, with $(\Delta C_D/C_D)_{tr} = 0.1$ as the altitude of a triangular distribution over a transition interval of $(\Delta h_{tr}/h_{tr}) = 0.06$. The asymmetrical component δ_{R_2} assumed a static margin $(\Delta X/L) = 0.07$, $\Delta C_{m_{tr}} = 0.001$ (equivalent to $\Delta \alpha_{tr} = 0.15$ deg), $(\Delta h_{tr}/h_{tr}) = 0.1$ and $(\Delta C_{m_{tr}} - \text{space-fixed})/\Delta C_{m_{tr}} = 0.5$. Equation 14 was used to calculate the results shown and must be consulted to scale the Fig. 12 results for δ_{R_2} to input values different than those above.

The statistical character of the symmetric component is such that it could well be included as an additional contributor to the conventional dispersion by root-sum-squaring. In that case, due to its modest magnitude compared to wind and

$$\Delta C_{m_{tr}} = 0.001, (\Delta X/L) = 0.07$$

$$(\Delta h_{tr}/h_{tr}) = 0.1, \left(\Delta C_{m_{tr}} \text{ SPACE FIXED} / \Delta C_{m_{tr}} \right) = 0.5$$

$$H = 22 \text{ kft}$$

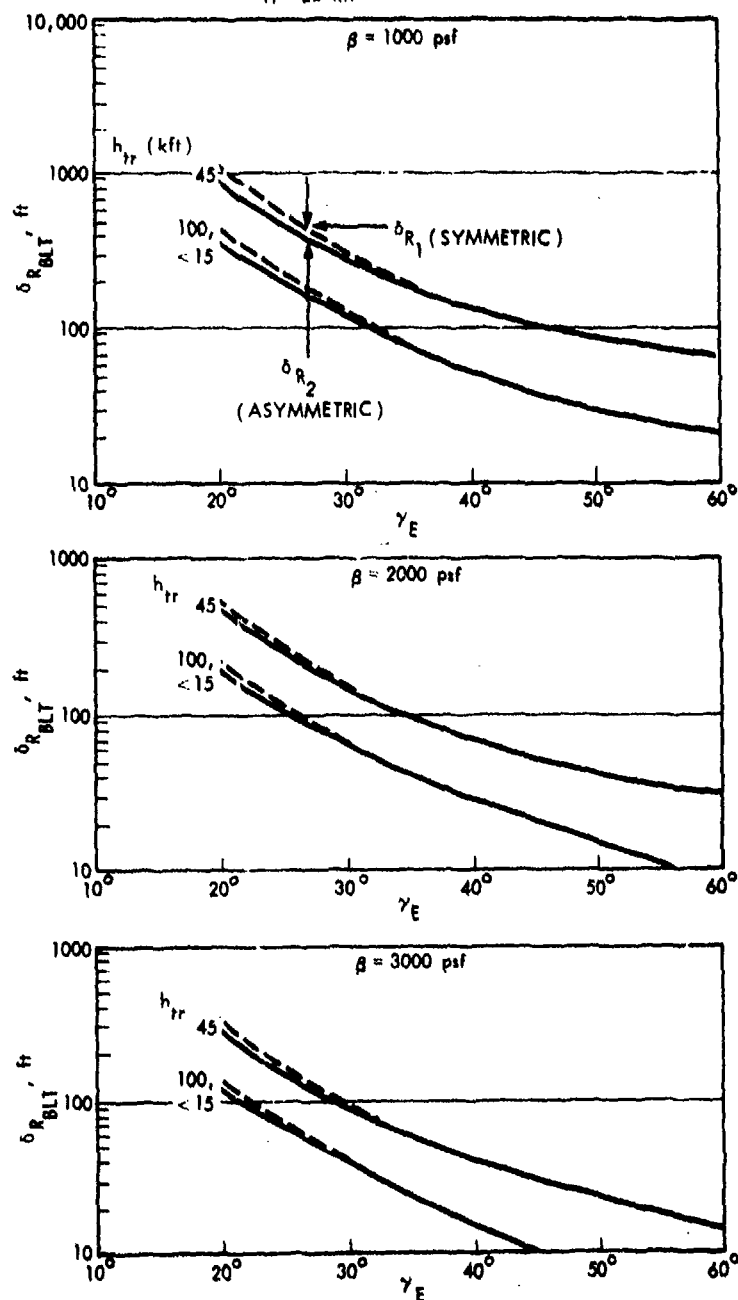


FIGURE 12. Maximum Rangewise Dispersion Due to Boundary Layer Transition at Several Altitudes Versus γ_E for Three β s at $V_E = 20$ kfps

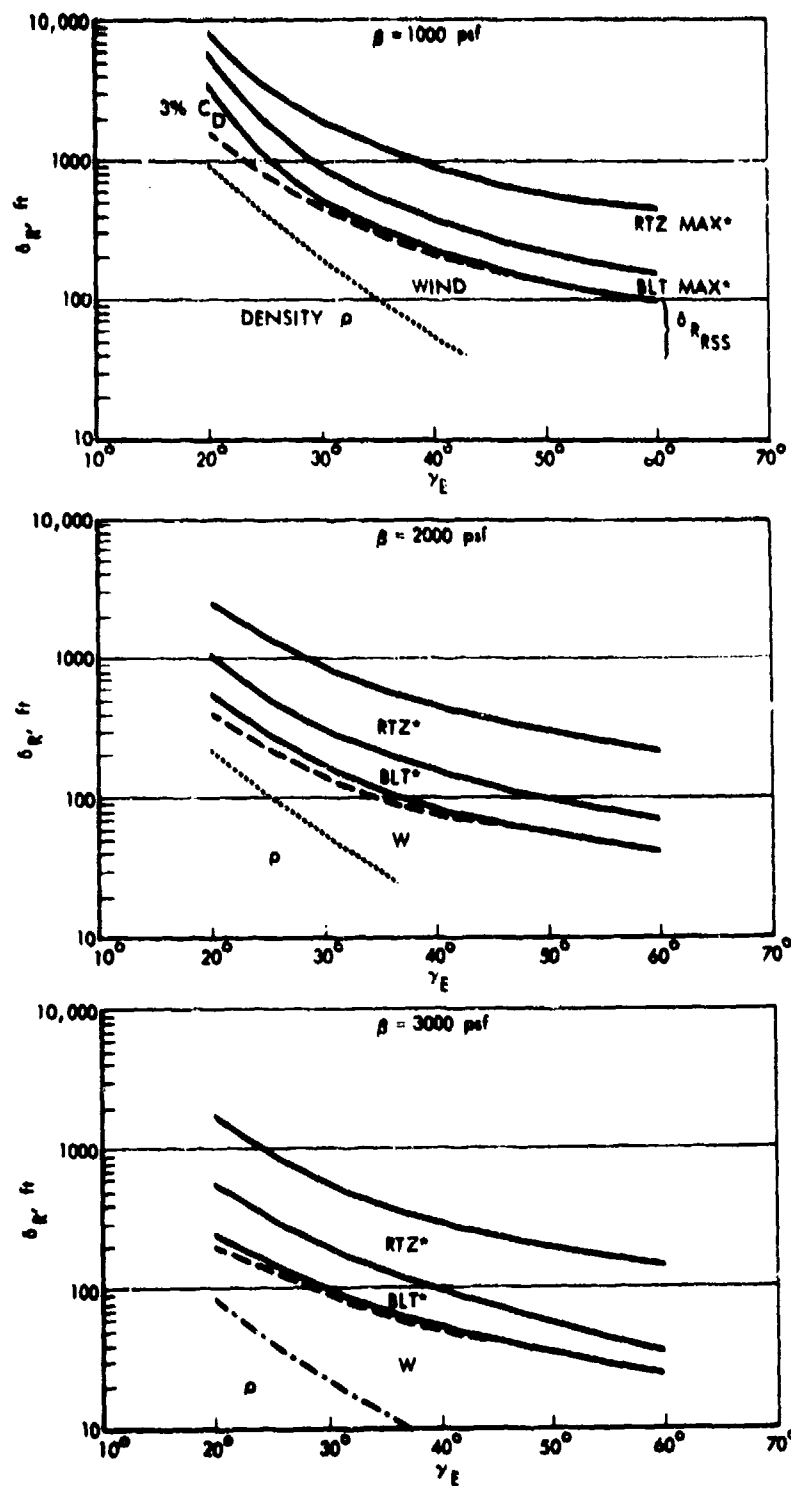
density contributors, it would hardly affect the magnitude of the conventional dispersion shown in Fig. 10. The symmetrical BLT dispersion component has therefore been neglected in subsequent calculations and comparisons.

As to the asymmetrical component, δ_{R_2} , its maximum range-wise dispersion values are not at all negligible but at least not as severe as the RTZ dispersions. Because of the elliptical impact pattern, the ratio of cross-range to rangewise dispersion is $|\sin \gamma_E|$, just as in the RTZ case. In addition, their statistical combination with all other components must be treated similarly to the probability treatment for $\delta_{R_{RTZ}}$ discussed in the preceding section. In this case, then, the probability of encountering or exceeding a given value of $\delta_{R_{BLT}}$ between zero and the maxima shown in Fig. 12 must be determined, including the probability of encountering one or more instances of the BLT asymmetry hanging up in the trajectory plane (in the RTZ case, zero roll can occur only once) combined with the probability of these given dispersion magnitudes coinciding with the semi-major axis (the trajectory) plane.

Comparing the magnitudes of the asymmetric BLT dispersion components with the previous two, one must keep in mind that the asymmetric forcing moment of $\Delta C_{m_{tr}} = 0.001$ can be different by one or more orders of magnitude and that the period of space-fixed direction may also be different from the $a = 0.5$ assumption. We simply do not have enough of a data base on this phenomenon to be more specific.

E. COMBINED DISPERSIONS

The three dispersion components calculated in preceding sections have been added together in Fig. 13 to show the trends of total range dispersions against reentry angle for the three ballistic coefficients at 20,000 fps reentry velocity.



*Maximum BLT and RTZ contributions added to RSSd wind/density/drag term.

13-4-75-17

FIGURE 13. Maximum Rangewise Dispersion Bounds Versus γ_E for Three β s at $V_E = 20$ kfps

This figure gives the sum of conventional + maximum asymmetric BLT + maximum RTZ components or $(\delta_{R_{RSS}} + \delta_{R_{BLT}} + \delta_{R_{RTZ}})$. Both BLT and RTZ components represent only the maximum value; the actual value must be determined from the specific probability considerations applying in individual cases. In addition, the combination of the conventional $\delta_{R_{RSS}}$ with the probabilistic $\delta_{R_{BLT}}$ and $\delta_{R_{RTZ}}$ must be done in a statistically consistent and meaningful manner, which cannot be done in this broad trend study.

Estimates of total rangewise dispersions for a reentry vehicle using Fig. 13 should recognize that both BLT and RTZ dispersion components can have any value within each respective band shown which may then be combined statistically (RSSd, for example) with the conventional component of dispersion.

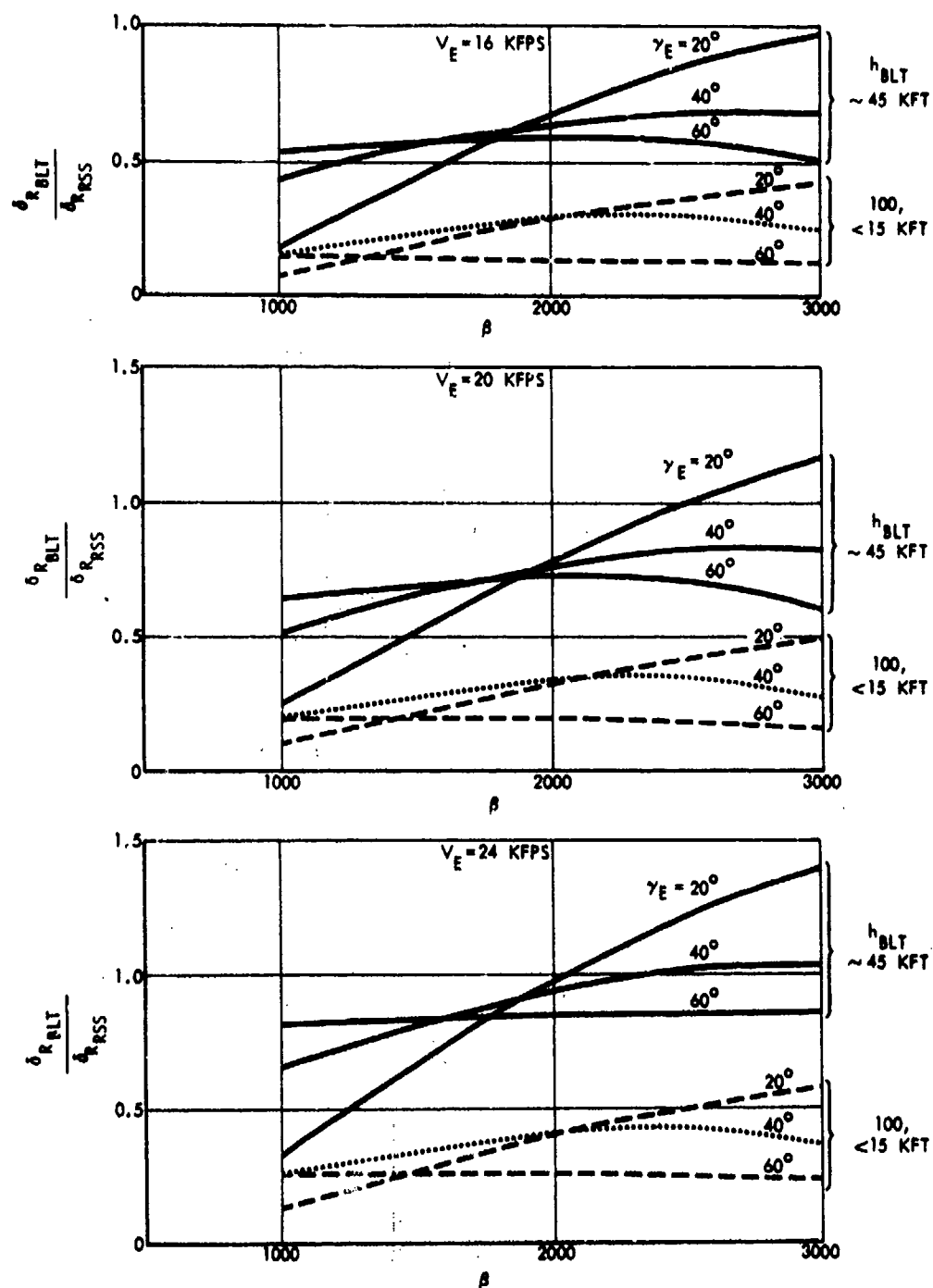
As to the total cross-range dispersion, it includes the cross-wind component of the wind dispersion and the BLT and RTZ erosion components, each multiplied by $\sin \gamma_E$.

F. DISPERSION RATIOS RELATIVE TO THE CONVENTIONAL DISPERSION

The magnitudes and trends of the dispersion components analyzed depend on the following basic parameters: ballistic coefficient β , reentry angle γ_E and velocity V_E , altitude of transition h_{BLT} , and altitude of roll-through-zero (or roll resonance) h_{RTZ} . The interaction between these parameters and $\delta_{R_{BLT}}$ and $\delta_{R_{RTZ}}$ becomes evident when these dispersion components are referenced to the conventional dispersion component.

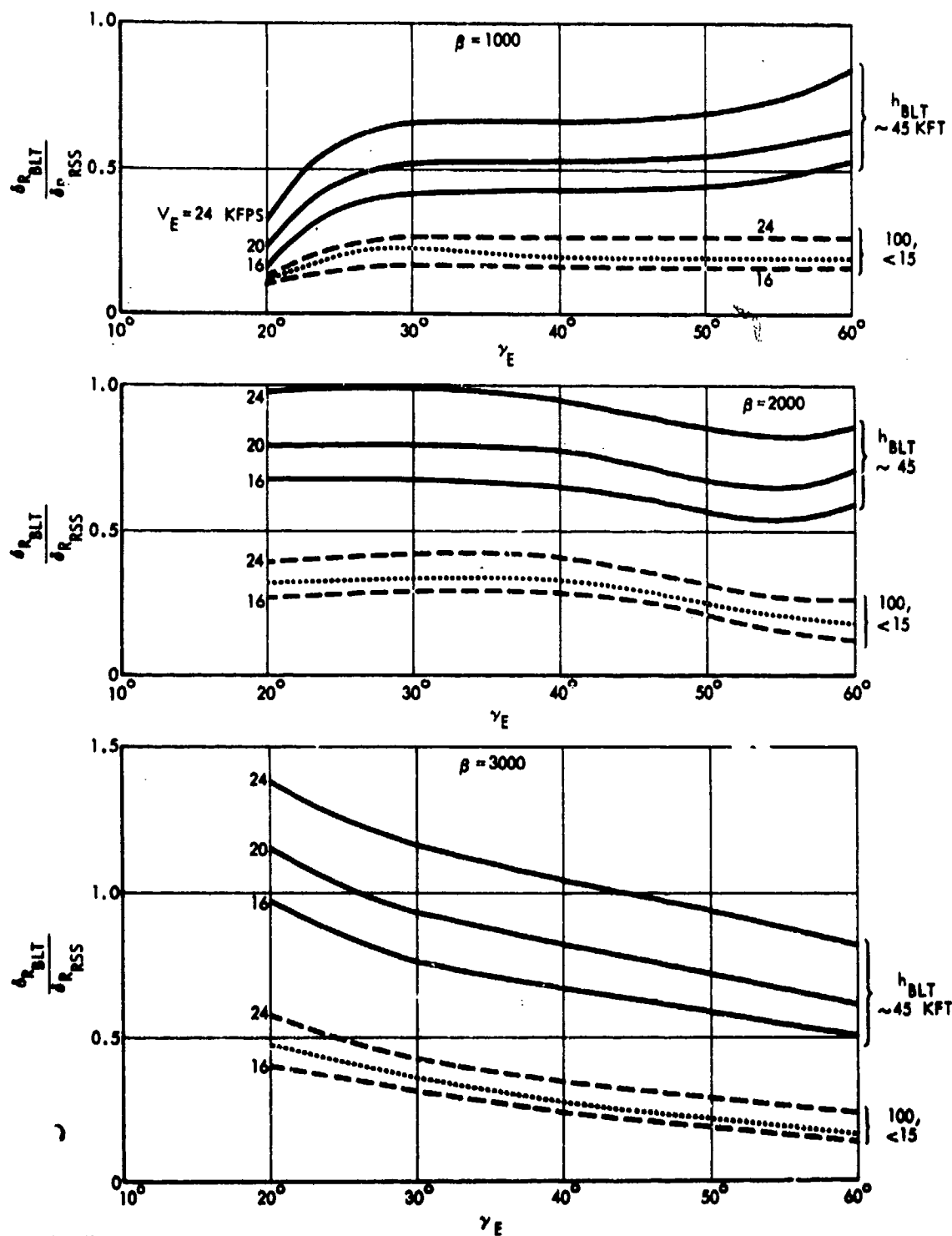
1. Boundary Layer Transition Component

For the boundary layer transition component, Figs. 14 and 15 show the ratios of $\delta_{R_{BLT}} / \delta_{R_{RSS}}$ plotted against β and γ_E , respectively, with γ_E and V_E as parameters. Boundary layer transition altitudes of around 45 kft (giving maximum $\delta_{R_{BLT}}$) and at 100 kft (and 15 kft and less) are shown on these figures.



12-8-75-21

FIGURE 14. Maximum BLT-Induced Dispersion Ratios Versus β for Various γ_E , V_E , and h_{BLT} Altitudes



12-8-75-20

FIGURE 15. Maximum BLT-Induced Dispersion Ratios Versus γ_E for Various β s, V_E s, and h_{BLT} Altitudes

Figure 14 shows this ratio to increase with increasing β , but there are ranges of ballistic coefficients over which it is essentially independent of reentry angle. At $V_E = 20$ kfps, for instance, the maximum ($\delta_{R_{BLT}} / \delta_{R_{RSS}}$) around $\beta \sim 1900$ psf is about 0.72 for all reentry angles between 20 and 60 deg. At $\beta = 1000$, however, this ratio is 0.65 for 60 deg, 0.25 for 20 deg, while at $\beta = 3000$ the γ_E trends reverse, giving ($\delta_{R_{BLT}} / \delta_{R_{RSS}}$) = 0.6 for 60 deg and 1.15 for 20 deg. Similar effects are evident throughout the range of parameters shown in Fig. 14.

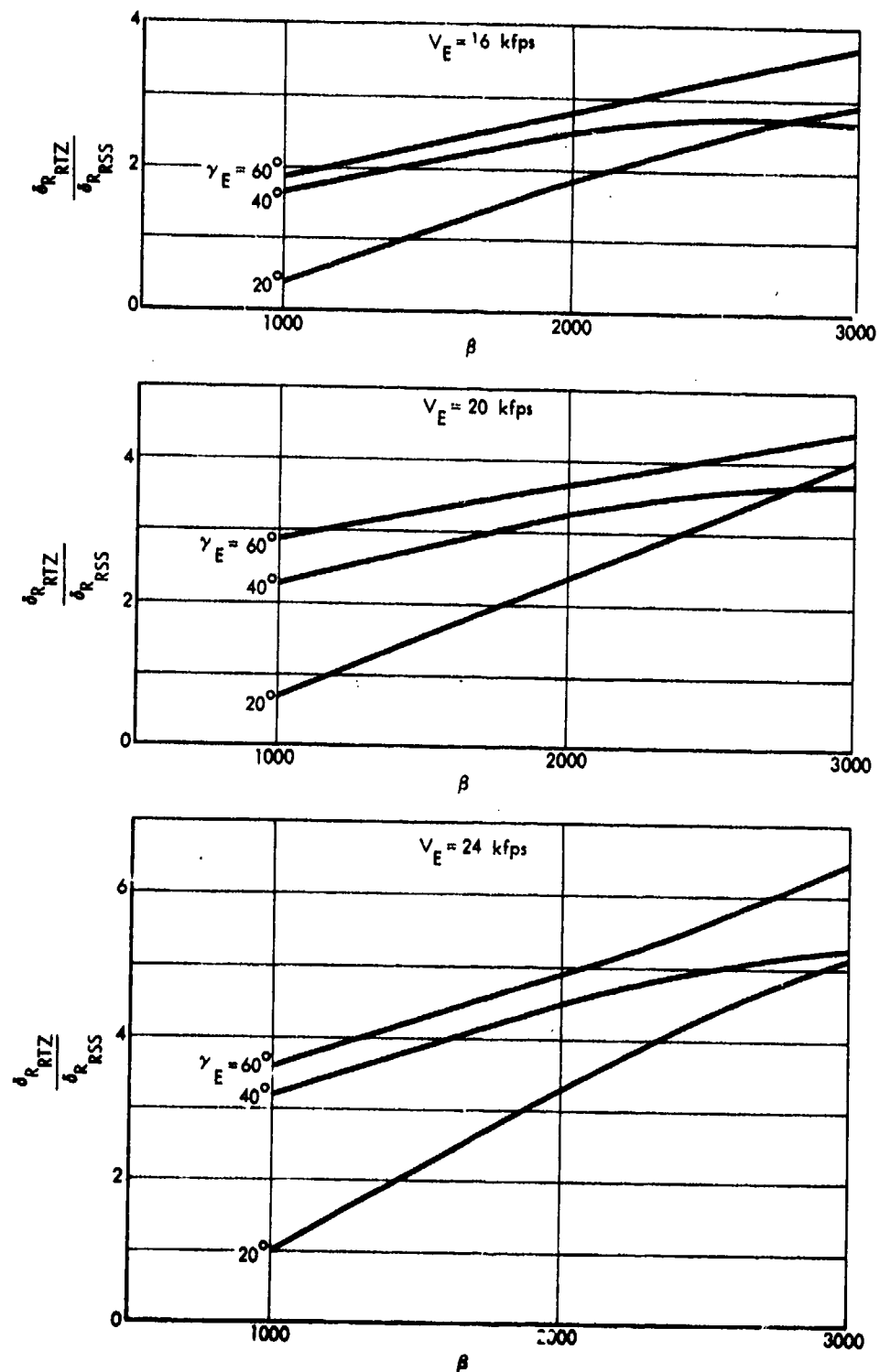
Figure 15 indicates that this dispersion ratio is fairly constant with reentry angle except for $\beta = 1000$ and 3000, while the effect of reentry velocity is very regular.

For the parameters investigated, the ($\delta_{R_{BLT}} / \delta_{R_{RSS}}$) ratios for transition at 100 kft or 15 kft and below run from around 0.1 to 0.5, while for $h_{BLT} \sim 45$ kft these ratios bound 0.5 to 1.0.

2. Roll-Through-Zero Component

Similarly, the values of $\delta_{R_{RTZ}}$ divided by $\delta_{R_{RSS}}$ are shown versus β in Fig. 16 and versus γ_E in Fig. 17 for the same range of parameters. In this case, only the roll-through-zero altitude of about 25 kft is shown, where $\delta_{R_{RTZ}}$ becomes maximum. In this case, the reentry angle shows a much more regular effect on this ratio except for some crossing of the 20- and 40-deg curves at very high betas (see Fig. 16), while the increase with increasing β is steeper than in the preceding case. However, the magnitude of the roll-through-zero dispersion ratios ranges from 2 to 6, confirming the need to prevent roll-through-zero from occurring.

Assuming that roll-through-zero has been eliminated, one may still experience roll resonance, in which case the dispersion ratios of Figs. 16 and 17 might be an order of magnitude lower, say from 0.2 to 0.6. Such magnitudes are comparable to the boundary layer transition ratios.



17-B-75-19

FIGURE 16. Maximum Roll-Through-Zero-Induced Dispersion Ratios Versus β for Various Reentry Conditions ($h_{RTZ} \sim 25$ kft)

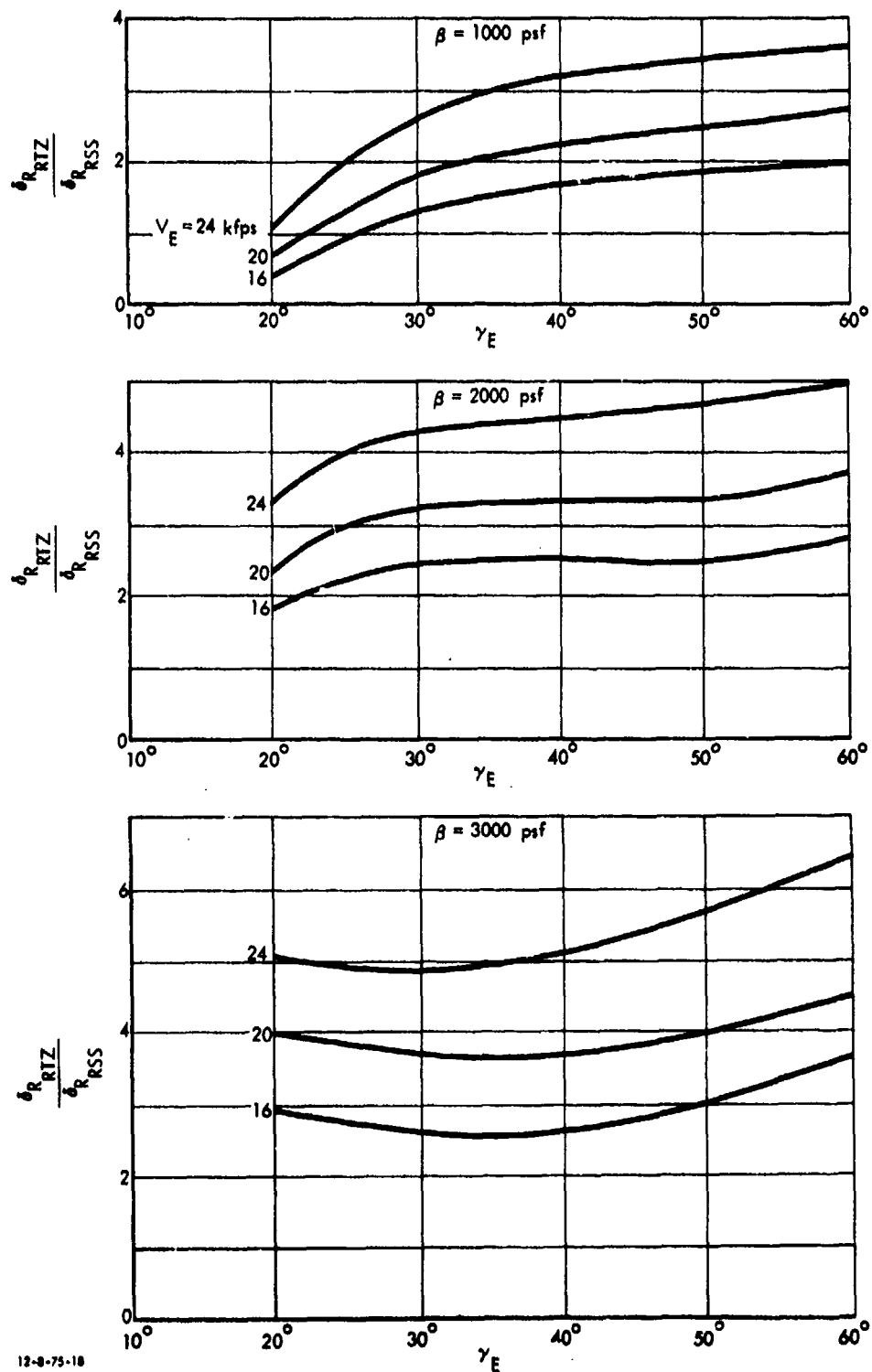


FIGURE 17. Maximum Roll-Through-Zero-Induced Dispersion Ratios Versus γ_E for Various β s and V_E s ($h_{RTZ} \sim 25$ kft)

REFERENCES

1. Personal discussions with ABRES personnel on 5 June 1975. Since this date, a document, Minutes for the Transition Dispersion Flight Data Analysis Technical Interchange Meeting (U), AS 75-03955, 19 August 1975, which summarizes these data, has been issued by the Aerospace Corporation.
2. M. V. Morkovin, "Open Questions - Transition to Turbulence at High Speeds," AFOSR-TR-70-1731, 1971 (UNCLASSIFIED).
3. J. Leith Potter, "Boundary Layer Transition on Supersonic Cones in an Aeroballistic Range," AIAA Paper 74-132, February 1974. (AIAA Journal, Vol. 13, No. 3, pp. 270-277, March 1975, gives condensed version of original paper, omitting the basic data of interest here.)
4. V. DiCristina, "Three-Dimensional Laminar Boundary Layer Transition on a Sharp 8° Cone at Mach 10," AIAA Journal, Vol. 8, No. 5, pp. 852-856, May 1970.
5. L. S. Glover, "Approximate Equations for Impact Dispersions Resulting From Winds and Deviations in Density," Journal Spacecraft & Rockets, Vol. 9, No. 7, pp. 483-484, July 1972.
6. L. S. Glover and J. C. Hagan, "The Motion of Ballistic Missiles," The Johns Hopkins University, Applied Physics Laboratory, TG 1164, July 1971 (UNCLASSIFIED).
7. A. Martellucci, "Analysis of Flight Test Ballistic Re-Entry Vehicle Boundary Layer Transition Data (U)," AIAA Joint Strategic Sciences Meeting, Vol. I, pp. 91-99, January 1974 (SECRET).
8. G. T. Chrusciel, "Analysis of R/V Behavior During Boundary Layer Transition," AIAA Paper 74-109, January 1974. (AIAA Journal, Vol. 13, No. 2, pp. 154-159, February 1975, contains condensed version of original paper, omitting most data used here.)

9. L. E. Ericsson, "Effect of Boundary-Layer-Transition on Vehicle Dynamics," Journal Spacecraft & Rockets, Vol. 6, No. 12, pp. 1404-1409, December 1969.
10. A. Martellucci and R. S. Neff, "Influence of Asymmetric Transition on Re-Entry Vehicle Characteristics," Journal Spacecraft & Rockets, Vol. 8, No. 5, pp. 476-482, May 1971.
11. R. G. Finke, "Reentry Vehicle Dispersion Due to Atmospheric Variations," IDA Research Paper P-506, August 1969 (UNCLASSIFIED).